NONLINEAR DYNAMIC BEHAVIOR OF SINGLE WALLED CARBON NANOTUBES WITH AN INITIAL GEOMETRIC IMPERFECTION USING SHELL ELASTICITY THEORY

A Thesis

Submitted to the Faculty of Graduate Studies and Research

in Partial Fulfillment of the Requirement

For the Degree of

Master of Applied Science

in

Industrial Systems Engineering

University of Regina

By

Roja, Bahramian

Regina, Saskatchewan

December, 2017

UNIVERSITY OF REGINA

FACULTY OF GRADUATE STUDIES AND RESEARCH

SUPERVISORY AND EXAMINING COMMITTEE

Roja Bahramian, candidate for the degree of Master of Applied Science in Industrial Systems Engineering**,** has presented a thesis titled, ***Nonlinear Dynamic Behavior of Single Walled Carbon Nanotubes with an Initial Geometric Imperfection Using Shell Elasticity Theory,*** in an oral examination held on September 5, 2017. The following committee members have found the thesis acceptable in form and content, and that the candidate demonstrated satisfactory knowledge of the subject material.

External Examiner:	Dr. Yongan Gu, Petroleum Systems Engineering
Supervisor:	Dr. Mohamed Ismail, Industrial Systems Engineering
Committee Member:	Dr. Liming Dai, Industrial Systems Engineering
Committee Member:	Dr. Rene Mayorga, Industrial Systems Engineering
Chair of Defense:	Dr. Lisa Watson, Faculty of Business Administration

*Not present at defense

Abstract

In this thesis, the nonlinear dynamic behavior of imperfect single-walled carbon nanotubes (SWCNTS) is investigated based on shell elasticity theory. According to the electronic microscope observations, most of the produced CNTS have imperfection and probably, there is not any ideal CNT without any defect. Therefore, in this study, the effect of imperfection on the nonlinear frequency and dynamic behavior is considered based on both classical and nonlocal shell elasticity theories and comparing it with the ideal CNT. The initial imperfection has been considered as a defect resulting from various kinds of defects. The imperfect SWCNT is modeled as an imperfect hollow shell. The Donnell's shell theory and Von-Karman's nonlinearity theory are used to obtain the governing equations. The Galerkin's method is implemented to transform partial differential equations into the ordinary differential equations of motion. The method of averaging is applied to solve the nonlinear equations of motion in the analytical calculations. The effects of the initial geometric imperfection, different aspect ratios, various nonlocal parameters, and the different wave numbers on nonlinear frequency and the softening or hardening behavior of the vibration are investigated. The results indicate the important influence of the nonlocal elasticity and an initial defect on the nonlinear behavior of SWCNT.

Keywords: Nonlinear Dynamic Behavior, SWCNT, Initial Geometric Imperfection, Donnell Shell Model, Averaging Method.

Acknowledgment

I would like to express my gratitude to my supervisor, Dr. Mohamed Ismail who gave me a chance to join to his research group and for his guidance and his patience.

I would also like to acknowledge Dr.Amr Henni for his time, help and advice during my study at the University of Regina.

With Special thanks to my husband for his support and encouragement during my study. Also, I must acknowledge my family for their support through my entire life.

I acknowledge the Faculty of Graduate Studies and Research and Faculty of Engineering and Applied Science for awarding me various scholarships and teaching assistantships during my study.

Table of Contents

List of Tables

List of Figures

List of Appendices

List of Nomenclature

L	Length of Carbon Nanotube
m	Axial Wave Number
n	Circumferential Wave Number
W_0	Imperfection Amplitude
$e_0.a$	Nonlocal Parameter
S	the fourth order elasticity tensor
T	Macroscopic Stress Tensor
$\sigma(x)$	Nonlocal Stress Tensor
$\lambda(\lvert x-x' \rvert, \mu)$	Nonlocal Modulus
$\lvert x-x' \rvert$	Euclidean distance
$\mu = \frac{e_0.a}{l}$	Material Constant
A(t)	Amplitude of Vibration
$\overline{A}$	Non-Dimensionless Amplitude
D	Flexural Rigidity
E	Elasticity Modulus
$\overline{F}$	Integrand Function
F	In-Plane Airy Stress Function
F_{Linear}	Linear Frequency
H	Thickness of Shell
$M_x, M_\theta, M_{x\theta}$	Moment Resultants

$N_x, N_\theta, N_{x\theta}$	Stress Resultants
R	Radius of Carbon Nanotube
u	Axial Movement
U	Strain Energy of the Shell
v	Circumferential Movement
w	Radial Movement
$\bar{\sigma}_x$ ، $\bar{\sigma}_\theta$ و $\bar{\sigma}_{x,\theta}$	Stress Components In x And θ Directions
$\bar{\varepsilon}_x, \bar{\varepsilon}_\theta, \bar{\gamma}_{x\theta}$	Strain Components at Arbitrary Points
$\varepsilon_x, \varepsilon_\theta, \gamma_{x\theta}$	Middle Surface Strain
$k_x, k_\theta, k_{x\theta}$	Curvature of the Middle Surface
υ	Poisson ratio
ρ	Mass Density of Shell
φ_i	Galerkin Weight Function
ω	Nonlinear Frequency
$\bar{\mu}$	Non-Dimensionless Nonlocal Parameter
ξ	Aspect Ratio
ε	Nonlinear Parameter
Ω	Frequency Ratio
x, θ, z	Axial, Circumferential and Radial Coordinates
Z	Distance of the Arbitrary Point of the Shell

List of Abbreviation

CNT: Carbon Nanotube

DWCNT: Double-Walled Carbon Nanotube

MD: Molecular Dynamic

MM: Molecular Mechanic

MWCNT: Multi-Walled Carbon Nanotube

ODE: Ordinary Differential Equations

PDE: Partial Differential Equations

SWCNT: Single-Walled Carbon Nanotube

TEM: Transition Electronic Microscope

1 Chapter one: Introduction

1.1. General Introduction

Among the elements found in nature, Carbon is an exception by having the ability to create structures and various forms. Carbon has four different forms which include graphite, diamond, nanotubes and fullerene. Graphite has a structure in which the atoms form a hexagon with each other in parallel planes. Diamond has very strong structural links that are interconnected in all directions, making it the hardest substance found in nature. Florin of 60 carbon atoms with 5 and 6-side arrangement is formed as a spherical established. If graphite layers are in the form of pipes, Carbon nanotube will be made [1].

Carbon nanotubes are the structures at the atomic level with the specific arrangement of the Carbon atoms. These hollow tubes are graphite or single graphene layer that rolled up in to cylindrical shape. Carbon nanotube diameter is about a few nanometers and its length is about micrometers [1].

Carbon nanotubes present superior mechanical and electrical properties which have always attracted scientists for excellent properties and a wide range of applications. This material which is stronger than Steel, lighter than Aluminum, more conductive than Copper [2][3] has many applications that key issues include sensors [4], transistors, electrochemical capacitors [5], composites , resonators, etc.

This structure was discovered in 1991 by "Sumio Iijima" During the study of the levels of graphite electrodes used in electric arc discharge [6].

According to the twisting angle of the Graphene layers (chirality), there are different types of nanotubes such as “chiral",”zigzag” and “Armchair” models (Figure 1-1).

As explained, the carbon nanotubes are created by rolling up the graphite layers. It could be structured by the vector C as a set of integers (*M, N*) and is based on two graphitic vectors a_1 and a_2 (Figure 1-2). The diameter is obtained by the following equation:

$$D = \frac{|C|}{\pi} = a(N^2 + NM + M^2)^{1/2} \qquad (1\text{-}1)$$

$$a = |a_1| = |a_2|$$

Here *a* is the graphite lattice constant. If in the structure of the nanotubes *M=N*, the structure is "armchair", *M=0* to be called the "zig-zag" and other type is called. "chiral” [7].

Based on the number of layers of carbon, carbon nanotubes are multi-walled carbon nanotubes (MWCNTs) and single-walled carbon nanotube (SWCNT) (Figure 1-2). Multi-walled nanotubes were discovered in 1993. This type (MWCNT) of nanotube production methods is different from single-walled. Multi-walled type has thicker walls and consist of several cylindrical coaxial who have a parted with each other about 0.34 nm (the distance between the layers of graphite). Single-walled carbon nanotubes behavior is a function of the bond between atoms. While, the behavior of multi-walled type is based on the interaction between different layers in addition to the interaction of atoms [3].

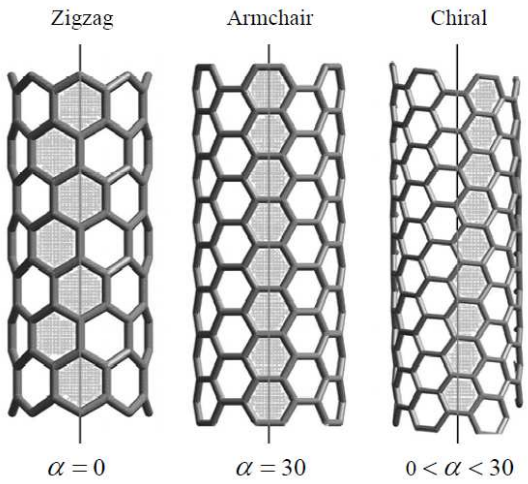

Figure 1-1: Structure of Armchair, Zig-Zag and Chairal

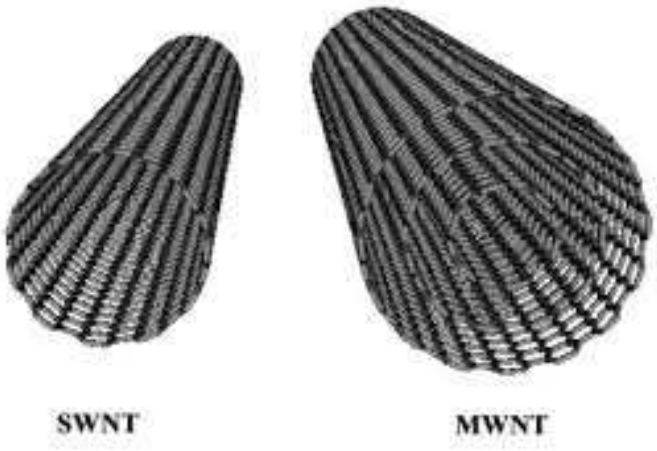

Figure 1-2: Cross-section of single-walled nanotubes, double-walled and multi-walled

1.2. Some Kinds of Carbon Nanotube Applications

Based on the unique properties, Carbon nanotubes have various interesting applications. In this section some important applications of carbon nanotubes are briefly introduced.

1.2.1. Sensors

Carbon nanotubes are used in the instruments with high sensitivity because of the small size and unique properties. One method for making such sensors, is taking advantage of the electrical properties of carbon nanotubes. Another interesting application of nanotubes as the sensors is using mechanical resonance frequency transmission to identify the absorbed molecules. With absorbing the external mass by the vibrated nanotubes, its natural frequency is reduced. Poncharal and colleagues [8] were able to estimate the mass of a particle attached to the end of cantilevered carbon nanotube by using the resonance frequency of carbon nanotube.

1.2.2. Transistors

Field Effect Transistor semiconductor can be built by single-walled carbon nanotubes. By applying a voltage to the gate electrode, carbon nanotubes will be changed from conductive state to insulating one. Nanotube transistors can be paired together, and be used as a logical switch for the computer's main components. These transistors can be used as well as silicon-based devices without much optimization [9].

1.2.3. Composites and Reinforced Polymers

Both SWCNTs and MWCNTs have good mechanical properties, because the structure of two-dimensional arrangement of carbon atoms in a graphite sheet makes the possibility

of big deformation out of the screen, while high strength carbon-carbon bond of the graphite sheet prevent any deformation or failure of the screen. This structural characteristic of nanotubes takes advantage of them to improve the hardness and strength of composite systems containing polymers [10].

1.2.4. Electrochemical Super Capacitors

Super capacitors have high capacity and have lots of applications for electronic tools. Capacitors are usually composed of two electrodes that are separated by an insulating material. The capacity of a super alloy is inversely proportional to the distance of the loads on the electrodes. Since this distance is in the order of nano meter (nm), carbon nanotube electrodes have very high capacities [5].

1.2.5. Medical Use

The first major application of nanotechnology in medical use is in the help provided in diagnosis and analysis of disease, drug delivery and as biocompatible materials in artificial organs. One of the most important applications of carbon nanotubes is in the transfer of fluids [11]. The fluid-filled carbon nanotube that looks like a small straw is used in drug delivery to specific points of the body which is used in the treatment of many diseases.

Cancer is a type of diseases in which cells grow up and duplicate abnormally, and it was the first diseases in which the application of carbon nanotubes in drug delivery has been applied. Now mainly cancer treatments include surgery, radiotherapy, and chemotherapy. These treatments are usually painful and can destroy normal cells as well as other side effects as well. Carbon nanotubes as drug delivery devices have the potential to target specific cancer cells with a lower dose than conventional medicine which can be equally

effective at killing cells. However, it does not damage healthy cells and cause side effects as well [12].

The technology of carbon nanotubes for drug delivery and treatment of cancer is growing rapidly. Now for drug delivery Liposome and Polymers are used, but carbon nanotubes have high loading capacity and good quality to penetrate host cells [13].

The thesis purposes to study and investigate the nonlinear dynamic behavior of an imperfect single-walled carbon nanotube (SWCNT) and comparing the results with an ideal carbon nanotube.

1.3. Defects and Disorder in Carbon Nanotubes

As defined above, Carbon nanotubes are nanostructures which have unique electrical and physical properties. Based on theoretical studies carried out, the electronic properties of an ideal carbon nanotube are a function of the diameter and chirality. However, in reality, and with existing production methods, the structure carbon nanotube rarely are perfect and without defect [14]. There are various kinds of defects such as topological defects, re-hybridization defect, incomplete defects and other defects [15]. Defects such as the blanks or holes in the structure of the nanotubes change their electrical and mechanical properties strongly.

1.3.1. Re-hybridization Defect

The carbon bonds change their situation between SP, SP^2 and SP^3. This phenomenon accrues locally during localized deformation instability under compressive loading. SP^2 hybridization is related to carbon bonds in graphite and SP^3 hybridization is related to the carbon bonds in diamond [15].

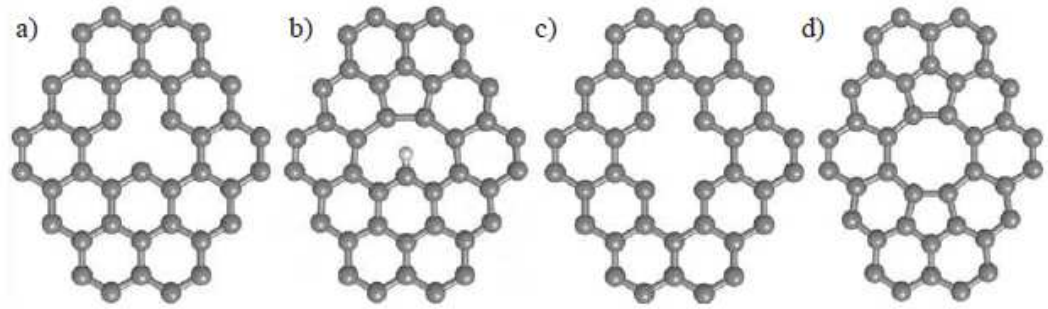

Figure 1-3: Blank or Holes Defect in Carbon Nanotube [14]

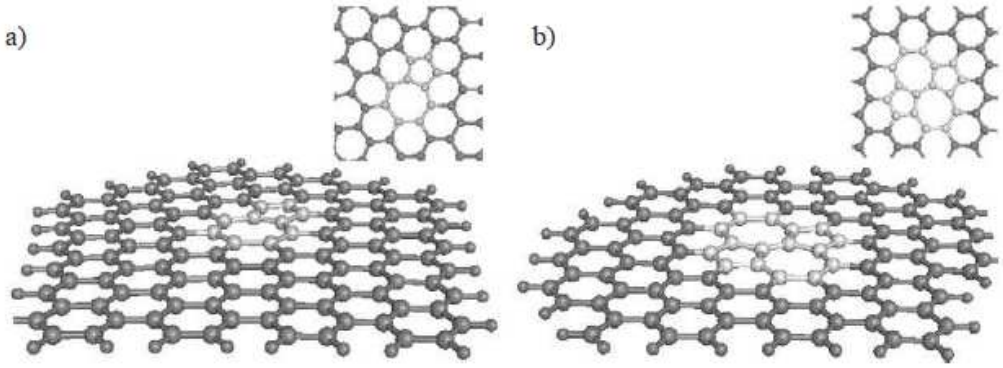

Figure 1-4: a) A single 5-7 defect b) A 5-7-7-5 Stone-Wales defect [14]

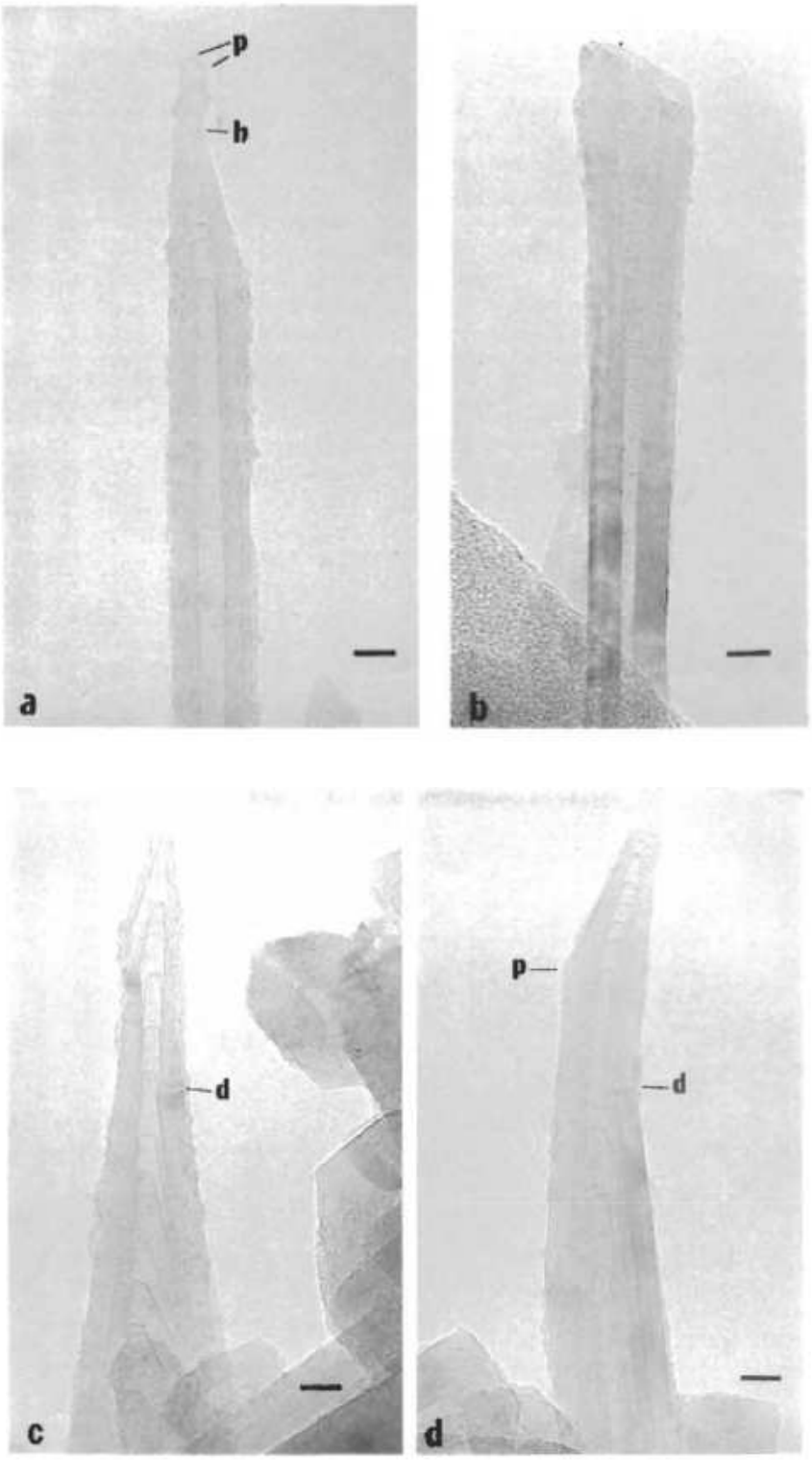

Figure 1-5: Examples of Carbon Nanotubes with various defects in their structures (P means pentagon, h means heptagon and d means dislocation) [15]

1.3.2. Topological Defect

The introduction of pentagons and heptagons ring size in the graphene sheet rather than hexagon type makes topological defect in a carbon nanotube [15]. One of the common types of this defect is Stone-Wales defect (SW 5/7/7/5) which is made by the rotation of atom bounds with 90 degree and makes a pair of pentagons or heptagons [14].

1.3.3. Blanks or Holes Defect

Defects related to incomplete hybrid structure include holes and dislocations. In this case, the smallest defect can be started by missing an atom or the existence of dislocations in a position which its size increases by increasing the number of absent atoms or presence of dislocations [14].

1.4. Defect Considered in This Research

Different defects are caused by the production of carbon nanotubes and the presence of these defects is inevitable. Ebbesen and Takada in 1995 showed that combination of different defects occurs during production of carbon nanotube, so it is not possible to separate these imperfections form one another. They explained in their study a few examples of the carbon nanotubes with several defects [15]. Also, Kinoshita et al. in 2013 showed the schematic of carbon nanotubes with multiple defects along the axial direction which made wavy shape, see (figure 1-6) [16].

In this present study, the widespread defect on the surface of SWCNT is considered, and the effects of this imperfection on the vibration of the carbon nanotube are discussed in detail. A widespread imperfection is a wide variety of defects including defects and combinations of them which makes waviness along the surface of the carbon nanotube.

SWCNT has been modeled the same as the cylindrical shell with an initial geometric imperfection. This initial imperfection has been considered as a simple model which represents the widespread defects on the carbon nanotube.

$$w_o(x,\theta) = W_0 \sin\left(\frac{m\pi x}{L}\right)\sin(n\theta) \tag{1-2}$$

This model has been by far in various studies [17]. Where W_0 is an imperfection amplitude, m is the axial wave number and equal to the number of half-waves along the shell, and n is the circumferential wave number.

1.5. Problem Statement

Because of the specific physical and electrical characteristics of carbon nanotubes, they have many applications in various industries that have attracted many researchers in recent years. However there are lots of researchers used theoretical methods to study the carbon nanotubes, most of them have considered the ideal carbon nanotubes. In reality, manufacturing an ideal carbon nanotube is too much expensive and inevitable. Defects have an influence on carbon nanotubes' properties such as strength or the electronic properties [15][18] and ignoring those leads to the difference between the experimental and the theoretical results. Hence to avoid the inaccuracy, it is highly predominant to consider imperfection during the study of carbon nanotubes.

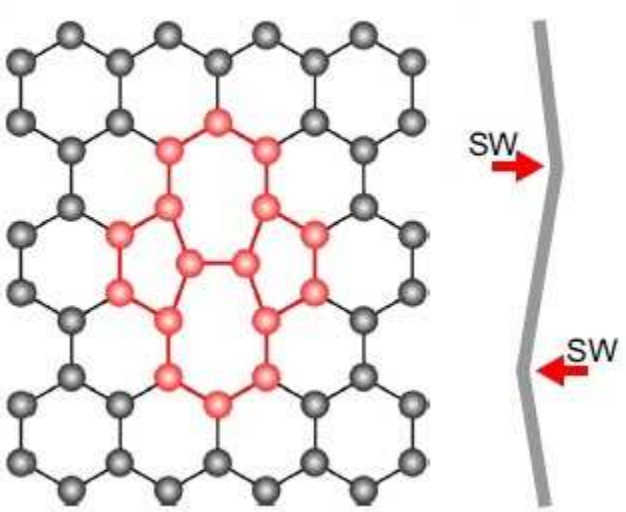

Figure 1-6: Schematic of carbon nanotube with SW defects [16].

1.6. Research Objectives

The purpose of this thesis is to study the nonlinear dynamic behavior of single-walled carbon nanotube with an initial geometric imperfection using continuum shell theory and considering an influence of imperfection on the vibration frequencies and dynamic behavior of single-walled carbon nanotube. To have the most accurate results with a good approximation with experimental results, following sub-goals have been considered:

- Almost all of the produced carbon nanotubes have different kinds of defects which affect their properties. Therefore, the main aim of this thesis is considering imperfection in carbon nanotubes. All of the previous works considered vacancies defect or the curved beam. However, in this research, a new kind of imperfection has been considered.

- The entire previous researches which employed continuum mechanic to study the defects in carbon nanotubes used beam elasticity theories. In the present research, shell elasticity has been used which is more accurate than beam elasticity theories.

- All the systems are nonlinear in reality, and scientists assumed linear systems to make them easier to study. In this thesis to have the perfect results and close to the experimental outcome, nonlinearity has been considered based on Von-Karman geometric nonlinearity theory.

- Another important factor is considering Eringen's nonlocal elasticity theory to consider the effect of small size and to increase the precision [19].

1.7. Thesis Outline

This thesis organized into five chapters and as follows:

The first chapter was specified to a general explanation about nanotechnology and carbon nanotubes. In this chapter, the molecular structure of carbon nanotubes, classification, common defects in structure and application of carbon nanotubes were studied.

In the second chapter, the literature review based on different types of modeling and with a focus on carbon nanotube with imperfection is discussed. In this chapter, various methods of modeling, including experimental and theoretical modeling are discussed, and shell method has been studied in more detail. Also, Eringen's nonlocal elasticity theory is studied in detail.

In the third chapter, the nonlinear dynamic analysis of perfect SWCNT based on continuum shell theory is considered. Strain-displacement equations have been extracted based on the nonlinear theory of Donnell's shell model. Galerkin's method and methods of averaging are used to solve the nonlinear equations of motion. Then, Eringen's nonlocal theory and Donnell cylindrical shell theory are used to study the perfect SWCNT.

The fourth chapter is devoted to study the effect of imperfection on the vibration frequencies and dynamic behavior of nanotubes. In this chapter, the influence of defects on the SWCNT based on the classical theory and the nonlocal elasticity theory is investigated and the results are compared with each other.

In the fifth chapter conclusions and recommendations are provided including the recommendations for future work.

2 Chapter two: Literature Review

In this chapter the literature review of previous research works based on various techniques of modeling is explained in detail. At first, experimental methods are described, and then the theoretical and analytical methods are studied. Each part includes the literature review based on the type of modeling. Also, the non-local elastic theory is discussed in detail in this chapter. Finally, the review of the previous works related to carbon nanotube with imperfection and the research plan is explained in detail.

2.1. Experimental Methods

Carbon nanotubes have small dimensions which cause great difficulties to study their mechanical properties. The main observed problem is a very small-scale phenomenon that requires very high precision microscopes. However, there are several types of laboratory researchers which have used an electron microscope and atomic force microscope to measure the mechanical properties of CNTs. Different loads are applied to CNTs, and the response is measured by using atomic force microscope. This method is useful for obtaining mathematical models. However, it is difficult to regenerate the model, also the response depends on the development of nano-size measuring device used for measurement which is a challenge itself.

Gao et al. [20] studied the vibration of single-walled carbon nanotube with the experimental method and Purcell et al. [21] studied the resonance frequency of multi-walled carbon nanotubes using electric field pulling method and found out that resonance frequency of carbon nanotube is in order of mega.

2.2. Discrete Modeling Approach (Methods of Molecular and Quantum Mechanics)

In the initial years of discovery, simulation of carbon nanotubes behavior was performed by using discrete methods such as molecular dynamics. Discrete methods will discuss temperature and strain of CNTs in a very small fraction of a second by taking into account the position of each atom, van der Waals bonds, and covalent bonds to other atoms. This works well in the case of elastic and inelastic and loading the material which is compatible with the experimental results. However, modeling the behavior of nanotubes according to their dimensions in this way, very time consuming and expensive and therefore, analyzing larger scale, for example, the composite scale is practically impossible [22]. There are two main methods in this kind of modeling, including methods of molecular dynamics (MD) and Ab-Initio method. Ab-Initio method is more accurate than molecular dynamic; however, it is computationally very difficult.

Zhou et al. [23] used molecular dynamic (MD) to study the mechanical behavior of carbon nanotube under tensile loading and they found out that it caused self-vibration in carbon nanotube which the vibration frequency is independent of the rate of strain.

2.3. Methods of Continuum Mechanics

Continuum mechanics is a proposed solution to model carbon nanotubes. Modeling of carbon nanotubes with this method is cheap, easy and very accurate. In this method, carbon nanotubes are modeled the same as beam or shell. Continuum mechanics techniques include modeling of nanotubes through Euler-Bernoulli elastic beam theory, the theory of Timoshenko elastic beam theory and continuum shell theories. Beam

theories are simpler to be used, and they are suitable for small deformation; however, shell theories are more complicated and suitable for larger deformation and complex distortion [24].

Continuum shell theories include Donnell's shell theory, Sander's shell theory, and Flugge's shell theory. These theories are used to obtain the equations of balance cylindrical shells. Donnell's shell theory is used more because of simple equations of motions. Both beam and shell theories include two various theories: "classical continuum methods" and "modified Continuum methods".

2.3.1. Classical Continuum Mechanics

As it was mentioned above, various beam or shell models are used for studying the CNTs. The results obtained by these models are compatible with the results obtained by experimental methods. In this continuum modeling of carbon nanotubes, the large scale and macro scale are addressed rather than taking into account the scale of atoms and fractions of a second. This approximation is applicable if the nanotube radius is significantly larger than the thickness of it [25].

Zhang et al. [26] studied transfer vibration of double-walled carbon nanotubes with Euler-Bernoulli beam theory and found out that the effect of axial load on the natural frequency of carbon nanotube is sensitive to the aspect ratios and vibration modes.

Aydogdu et al. [27] Studied the vibration and buckling of carbon nanotube under axial load using Timoshenko beam theory and found out that axial load affected natural frequency. The increment of compressive load decreases the natural frequency; however, the tensile load will increase the natural frequency.

Sun et al. [28] used Donnell shell theory to consider the vibration of multi walled carbon nanotubes under axial load and found out that resonant frequencies are related to tension and compression axial load; however, vibration modes are independent of axial load.

Yan et al. [29] studied non-coaxial vibration of multi-walled carbon nanotube using classical Donnell shell theory and found out that resonant frequencies decreased at the presence of fluid.

Ansari et al. [30] studied nonlinear vibration of embedded multi-walled carbon nanotube using Euler-Bernoulli beam theory. They found out that nonlinear frequency was decreased by increasing the aspect ratios.

Soltani et al. [31] studied nonlinear vibration of single walled carbon nanotube using the classical shell theory. They found out that the degree of nonlinearity is directly related to wall thickness and radius of SWCNT.

2.3.2. Modified Continuum Mechanics

As the size of nano material is too tiny and the space between the atomic lattices is very important, hence homogenization of CNTs to a continuum model is not very correct. It means that the classical model is questionable at very small scales. Therefore, it is necessary to advance the models and consider the effects of nano scale. Great efforts have been made to develop better ways of modeling for having the much similar results to the molecular dynamics. A hybrid model (composition of atomic and continuum mechanic) is directly entered the atomic potential in to the continuum analysis which obtains by equating the molecular potential energy with strain energy of nano structure in the continuum model.

Zhang et al.[32][33] used the hybrid model to study the carbon nanotubes.

Other theories of continuum mechanics are based on nonlocal elasticity theory expressed by Eringen [34][35]. In this theory which contains information about the large atomic force, the effects of nano scale can be entered as a material parameter in to the equations. The first use of nonlocal continuum theory in nanotechnology was conducted by Peddieson [36].

2.4. Modified Continuum Mechanics based on Nonlocal Elasticity Theory

Due to the small size of CNT, the effects of dimension are significant and the use of classical continuum mechanics theories is questionable. Hence, small discrete scales of material properties cannot be ignored. Nonlocal elasticity theory was expressed by Eringen [35][37], on the assumption that the stress at any point is a function of strain on all other points. As a result, continuum mechanics using nonlocal theory can fully explain the mechanical condition of CNTs. Sudak [38] considered column buckling behavior of nanotubes Peddieson [36] introduced a continuum nonlocal model at the nano scale. Then, other related works have been done on the mechanical properties of CNTs based on this theory.

Eringen's nonlocal elasticity theory is based on the assumption that the stress at any point is a function of strain on all the other points. Therefore, nonlocal stress tensor at the point x, not only related to the strain at x but also depends on the strain at all other points x' and can be expressed as follows:

$$\sigma(x) = \int_v \lambda(|x - x'|, \mu).\bar{t}(x')dV(x'), \forall x \in V \qquad (2\text{-}1)$$

Where t is macroscopic stress tensor, $\lambda(|x-x'|,\mu)$ is the nonlocal modulus which $|x-x'|$ is the Euclidean distance $\mu=\frac{e_0.a}{l}$ (a is internal characteristic length and l is an external characteristic length) material constant which $e_0.a$ obtains by experiment or by matching dispersion curves of plane waves with those of atomic lattice dynamics [39]. Equation (2-1) in a differential form and in the two dimensional nonlocal elasticity can be written as:

$$(1-(e_0.a)^2.\nabla^2)\sigma=\bar{t} \qquad (2\text{-}2)$$

When the nonlocal parameter $e_0.a$ becomes zero, the nonlocal elasticity changes to the classical (local) elasticity. Based on the Hooke's law, stress tensor is related to strain which can be expressed as:

$$\bar{t}=S: \qquad (2\text{-}2)$$

Where S is the fourth order elasticity tensor and ':' indicates the double dot product [35][37].

Ke et al. [40] studied nonlinear vibration of double-walled carbon nanotube embedded in an elastic medium based on nonlocal Timoshenko beam theory. They found out that increasing the nonlocal parameter decreased the linear and nonlinear frequency, but

increased the frequency ratio. Also, increasing the spring constant increased both linear and nonlinear frequency, but reduced frequency ration.

Ansari et al. [19] used shell theory and nonlocal elasticity theory to study the vibration of single walled carbon nanotube. They used radial interpolation method for solving the equations of motion and showed that nonlocal parameter has a significant effect on resonant frequency.

Fang et al. [41] used nonlocal Euler-Bernoulli beam theory to study the nonlinear vibration of double-walled carbon nanotubes. They used harmonic balance method and Davidon–Fletcher–Powell method to solve the nonlinear equations of motion. They found out that nonlocal parameter, aspect ratios play an important role in the nonlinear vibration of carbon nanotubes.

Ghorbanpour et al. [42] studied nonlinear vibration of double-walled carbon nanotube conveying fluid by suing nonlocal shell theory. They used Hamilton's principle for the derivation of equations of motion. They found out that nonlocal parameter reduced the frequency ratio and critical flow velocity.

Soltani et al. [43] studied nonlinear vibration of single-walled carbon nanotube by suing nonlocal shell theory. They showed that nonlocal parameter found different resonance frequencies compare to the classical theory.

Wang et al. [44] Studied nonlinear vibration of embedded carbon nanotube in a viscous elastic medium based on nonlocal Euler beam theory, and found out that nonlocal parameter has a significant impact on positive bifurcation of short carbon nanotubes.

2.5. Literature Review with Focus on Carbon Nanotube with Imperfection

At first Carbon nanotubes were considered as a perfect cylindrical shell and without any defects .However, an electron microscope showed that very little of the carbon nanotubes are produced without defects and almost most of the carbon nanotubes have various kinds of defects in their structures [15]. In the case of mechanical behavior of nanotubes, sometimes there is much difference between the results predicted and the experimental results. Part of the difference can be attributed to the accuracy of test systems and part of it is due to different structures between the real structures and the ideal theoretical ones. Now due to limited laboratory conditions, defects in a carbon nanotube are common. With regard to this issue in recent years, many researchers were focused on investigating the behavior of carbon nanotubes with defects.

Hirai et al. [45] used molecular dynamics to investigate an effect of vacancies on the vibration and mechanical behavior of carbon nanotubes. The results show that resonance frequency (bending rigidity) increased by increasing the number of defects. Also, tensile strength and buckling significantly affected even by one single defect.

Dumitrica and Yakobson [46] studied the effect of temperature and loading rate over the stone-wales defect (5/7/7/5).

Mielke et al. [47] used quantum mechanics and molecular mechanics (MM) to consider the influence of vacancy on the tensile behavior of carbon nanotube. They show that the hole defect in carbon nanotube leads to a small reduction in tensile stiffness and a significant reduction in the strength of nanotubes.

Zhang et al. [48] used molecular mechanic (MM) coupling with birding MM and Finite crystal elasticity to consider the defects in carbon nanotube behavior. The results also indicate a slight decrease in tensile hardness and a significant reduction in the strength of the nanotube. For example for nanotubes (10, 0) due to the vacancies, tensile strength reduced from 87.9 Gpa to 64.4 Gpa.

Tserpes and Papanikos [49] studied Stone-Wales defect effect on tensile behavior and failure of single-walled nanotubes. zig-zag, chiral and armchair by using molecular mechanics; the results show the existence of defects in carbon nanotubes with different chirality make different results for properties mechanical of nanotubes.

Shen and Zhang [50] considered buckling and post-buckling of DWCNT with a defect and under axial and radial mechanical load. They considered the defect as a dimple on nanotube wall and used shell theory and non-local theory of modeling of the carbon nanotube. As a result of the study, the effect of cavity defects on nanotubes post buckling under the combined radial, and axial loads and temperature effect is discussed.

Shen and Zhang [51] in another study, have considered the effect of a vacancy on DWCNT under torsional load and used nonlocal elasticity theory in this research too.

Farshidinfar and Soltani [52] considered the nonlinear flow-induced vibration of SWCNT with geometric imperfection. They considered that SWCNT has a slight curvature. They used Euler-Bernoulli beam theory for modeling the carbon nanotube and used the method of multiple scales to solve the nonlinear equations. They showed that nonlinear flow induced frequency ratio decreased by increasing an imperfection in SWCNT.

Wang et al. [53] used Timoshenko beam theory to investigate the nonlinear vibration of SWCNT with geometric imperfection and under harmonic load. They considered SWCNT as a curved beam, and showed the effects of nonlocal parameter, wave numbers and elastic medium constants on the nonlinear behavior of SWCNT. They show that the effects of the mentioned parameters cannot be ignored for investigation of the behavior of SWCNT.

Mohammadi et al. [54] considered post-buckling instability of SWCNT with geometric imperfection. They considered SWCNT as a curved beam, and used Euler-Bernoulli beam and nonlocal theory to model the SWCNT. They showed that nonlocal parameters have a significant influence on post buckling of SWCNT and by using the nonlocal theory the behavior of SWCNT is similar for both straight and curved nanotube.

Rafiee et al. [55] considered the nonlinear dynamic stability of piezoelectric functionally graded carbon nanotube. They used shear deformation plate theory and Von-Karman geometric nonlinearity. Results of the research showed that initial geometric imperfection and increasing of the temperature have a significant effect on the stability of carbon nanotube.

Wu et al. [56] used shear deformation beam theory and Von-Karman nonlinearity theory to investigate the nonlinear vibration of the carbon nanotube. The results showed that nonlinear vibration of the beam is extremely sensitive to imperfection

Eshraghi et al. [57] used Timoshenko beam theory and nonlocal elasticity theory to study imperfection sensitivity of nonlinear vibration of curved SWCNT. They found that imperfection value and location has a large influence on linear and nonlinear vibration and higher imperfection increases the frequency of SWCNT.

2.6. Research Plan

In the recent years, simulation of the dynamic behavior of carbon nanotube, using the vibration measurement to describe the mechanical properties of carbon nanotubes and studying the nano resonators have attracted researchers and engineers. It is highly predominant to study the frequency and vibration amplitudes of carbon nanotubes in order to manufacture various devices such as oscillators or sensors. Furthermore, transport properties of carbon nanotubes containing fluids are sensitive to the frequencies and the vibration shape modes.

Most of the researchers show that scientists simulate CNTs as an entirely perfect structure; however, transition electronic microscopes (TEM) show that CNTs have waviness along their length which significantly influences their mechanical and electronically properties [58]. Based on the literature review, there are a few types of researches which studied the effect of the imperfection on the behavior of CNTS by using the continuum mechanics. Also, most of the works have been done before, concentrated on the investigation of bucking, post-buckling, and stability of CNTs. A few papers have addressed the nonlinear behavior of carbon nanotubes, and all of them used the beam theories for the modeling of CNTs. Moreover, all of them considered vacancies defect or the curved beam.

Due to lack of research works in this area especially those based on shell elasticity theory, the motivation of this work is to consider the nonlinear dynamic behavior of single walled carbon nanotube with an initial geometric imperfection using the shell elasticity theory. This initial imperfection has been considered as a simple model which represents the widespread defects on the carbon nanotube Therefore, Donnell' shell

theory is used for modeling of SWCNT and Eringen's nonlocal elasticity theory is applied to have more accurate results.

3 Chapter Three: Nonlinear Dynamic Analysis of an Ideal SWCNT

In this chapter nonlinear dynamic of perfect SWCNT is investigated. This chapter is composed of two sections. In the first part perfect SWCNT is modeled based on the classic shell theory. In the second part, SWCNT was modeled based on the nonlocal shell theory and the effect of various parameters on the frequency of SWCNT is studied and compared with the classical theory.

3.1. Classical (Local) Donnell's Shell Theory

SWCNT is considered as a thin cylindrical shell with radius R, thickness h and length L , see figure 3-1. Cylindrical coordinates (O: x, r, θ) selected to be the origin of coordinates on the surface of the shell. The displacements of the shell which are shown by w, v, u represent the movement in the direction of radial, circumferential and axial respectively. When the shell deflection w is in the same order of the magnitude of the shell thickness h, the linear theories become inaccurate; hence, a theory of large deflections (Von-Karman theory) is developed in cylindrical coordinates. In Donnell's nonlinear theory, only nonlinear terms that depend on w are maintained and all other nonlinear terms are ignored [59][60].

Governing equations are achieved based on the energy methods and the principal of the virtual works and the variation technique. The elastic strain energy U of a circular cylindrical shell is given by [61]:

$$U = \frac{1}{2}\iiint (\bar{\sigma}_x \bar{\varepsilon}_x + \bar{\sigma}_\theta \bar{\varepsilon}_\theta + \bar{\sigma}_z \bar{\varepsilon}_z + \bar{\tau}_{x\theta} \bar{\gamma}_{x\theta} + \bar{\tau}_{z\theta} \bar{\gamma}_{z\theta} + \bar{\tau}_{zx} \bar{\gamma}_{zx}) dx R(1 + \frac{z}{R}) d\theta dz \tag{3-1}$$

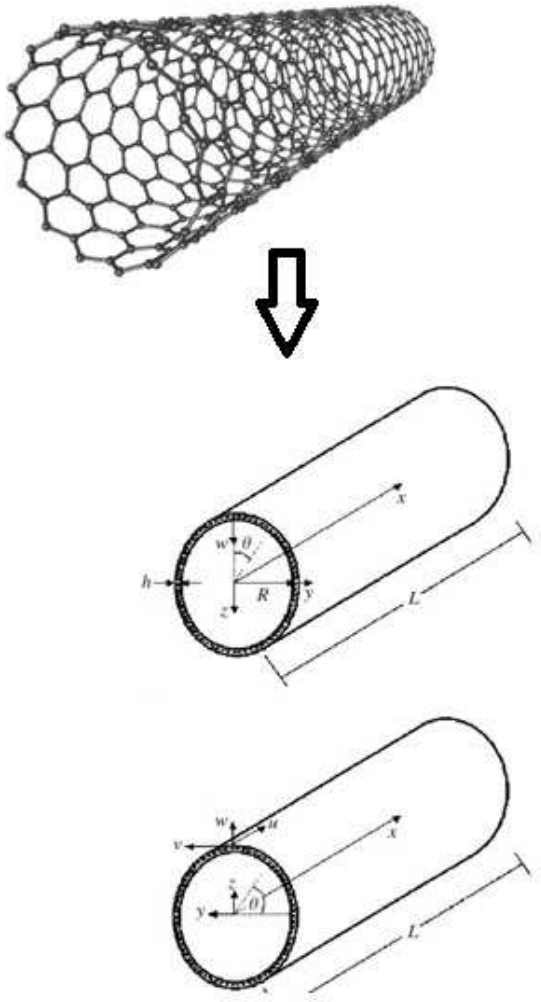

Figure 3-1: SWCNT as a thin cylindrical shell.

Based on the Love's first approximation [62], $\bar{\sigma}_z, \bar{\gamma}_{zx}$ and $\bar{\gamma}_{z\theta}$ will be omitted, and due to the proportion of $\frac{Z}{R}$ is smaller than 1, therefore $1+\frac{z}{R}\longrightarrow 1$.

With regard to the cases mentioned above the strain energy is simplified to:

$$U=\frac{1}{2}\iiint(\bar{\sigma}_x\bar{\varepsilon}_x+\bar{\sigma}_\theta\bar{\varepsilon}_\theta+\bar{\tau}_{x\theta}\bar{\gamma}_{x\theta})dxRd\theta dz \tag{3-2}$$

The Kirchhoff stresses for a homogeneous and isotropic material are given by

$$\begin{aligned}\bar{\sigma}_x&=\frac{E}{(1-\upsilon^2)}(\bar{\varepsilon}_x+\upsilon\bar{\varepsilon}_\theta),\\ \bar{\sigma}_\theta&=\frac{E}{(1-\upsilon^2)}(\bar{\varepsilon}_\theta+\upsilon\bar{\varepsilon}_x),\\ \bar{\tau}_{x\theta}&=\frac{E}{2(1+\upsilon)}\bar{\gamma}_{x\theta}.\end{aligned} \tag{3-3}$$

where $\bar{\sigma}_x$, $\bar{\sigma}_\theta$ و $\bar{\sigma}_{x,\theta}$ are the stress components in x and θ directions and E is the elasticity modulus, and υ is the Poisson ratio.

By substituting Eq. (3-3) in to Eq. (3-2), the elastic strain energy is rewritten as

$$U=\frac{1}{2}\iiint\frac{E}{(1-\upsilon^2)}(\bar{\varepsilon}_x^2+2\upsilon\bar{\varepsilon}_x\bar{\varepsilon}_\theta+\bar{\varepsilon}_\theta^2+\frac{(1-\upsilon)}{2}\gamma_{x\theta}^2)dxRd\theta dz. \tag{3-4}$$

The strain components $\bar{\varepsilon}_x, \bar{\varepsilon}_\theta$ and $\bar{\gamma}_{x\theta}$ are at arbitrary points of shell related to the middle surface strains $\varepsilon_x, \varepsilon_\theta$ and $\gamma_{x\theta}$ as well as the changes in the curvature of the middle surface k_x, k_θ and $k_{x\theta}$ [59]

$$\bar{\varepsilon}_x = \varepsilon_x + zk_x,$$
$$\bar{\varepsilon}_\theta = \varepsilon_\theta + zk_\theta, \tag{3-5}$$
$$\bar{\gamma}_{x\theta} = \gamma_{x\theta} + zk_{x\theta}.$$

Where z is the distance of the arbitrary point of the shell from the middle surface. The Von-Karman theory is used, and the following expression for the middle surface strains and the changes in the curvature and torsion of the middle surface are written as [59]

$$\varepsilon_x = \frac{\partial u}{\partial x} + \frac{1}{2}\left(\frac{\partial w}{\partial x}\right)^2,$$
$$\varepsilon_\theta = \frac{1}{R}\frac{\partial v}{\partial \theta} + \frac{w}{R} + \frac{1}{2R^2}\left(\frac{\partial w}{\partial \theta}\right)^2, \tag{3-6}$$
$$\gamma_{x\theta} = \frac{1}{R}\frac{\partial u}{\partial \theta} + \frac{\partial v}{\partial x} + \frac{1}{R}\left(\frac{\partial w}{\partial \theta}\right)\left(\frac{\partial w}{\partial x}\right).$$

$$k_x = -\frac{\partial^2 w}{\partial x^2},\ k_\theta = -\frac{\partial^2 w}{\partial \theta^2}, k_{x\theta} = -\frac{2}{R^2}\frac{\partial^2 w}{\partial \theta \partial x}. \tag{3-7}$$

By substituting Eq. (3-5) and Eq. (3-7) in Eq. (3-4) and integrating concerning z, an integrand function is obtained as:

$$\overline{F} = \frac{CR}{2}(\varepsilon_x^2 + \varepsilon_\theta^2 + 2\upsilon\varepsilon_x\varepsilon_\theta + \frac{(1-\upsilon)}{2}\gamma_{x\theta}^2) + \frac{RD}{2}(k_x^2 + k_\theta^2 + 2\upsilon k_x k_\theta + \frac{(1-\upsilon)}{2}k_{x\theta}^2).$$

$$D = \frac{Eh^3}{12(1-\upsilon^2)} \tag{3-8}$$

$$C = \frac{Eh}{1-\upsilon^2}$$

Where D is the flexural rigidity. With the above-mentioned formula, strain energy is defined as:

$$U = \iint \overline{F}(u_{,x}.u_{,\theta}, v_{,x}, v_{,\theta}, w_{,x}, w_{,\theta}, w_{xx}, w_{\theta\theta}, w_{x\theta})dxd\theta. \tag{3-9}$$

Based on the energy method, principal of the virtual works and the variation technique, the Euler equations are written as:

$$\frac{\partial\overline{F}}{\partial u} - \frac{\partial}{\partial x}(\frac{\partial\overline{F}}{\partial u_{,x}}) - \frac{\partial}{\partial\theta}(\frac{\partial\overline{F}}{\partial u_{,\theta}}) = 0,$$

$$\frac{\partial\overline{F}}{\partial v} - \frac{\partial}{\partial x}(\frac{\partial\overline{F}}{\partial v_{,x}}) - \frac{\partial}{\partial\theta}(\frac{\partial\overline{F}}{\partial v_{,\theta}}) = 0, \tag{3-10}$$

$$\frac{\partial\overline{F}}{\partial w} - \frac{\partial}{\partial x}(\frac{\partial\overline{F}}{\partial w_{,x}}) - \frac{\partial}{\partial\theta}(\frac{\partial\overline{F}}{\partial w_{,\theta}}) + \frac{\partial^2}{\partial x^2}(\frac{\partial\overline{F}}{\partial w_{,xx}}) + \frac{\partial^2}{\partial\theta^2}(\frac{\partial\overline{F}}{\partial w_{,\theta\theta}}) + \frac{\partial^2}{\partial x\partial\theta}(\frac{\partial\overline{F}}{\partial w_{,x\theta}}) = 0.$$

The stress and moment resultants are written by using Eq. (3-3) as follow:

$$N_x = C(\varepsilon_x + \upsilon\varepsilon_\theta)\,, M_x = D(k_x + \upsilon k_\theta)\,.$$

$$N_\theta = C(\varepsilon_\theta + \upsilon\varepsilon_x)\,, M_\theta = D(k_\theta + \upsilon k_x)\,. \qquad (3\text{-}11)$$

$$N_{x\theta} = C\frac{(1-\upsilon)}{2}\gamma_{x\theta}\,, M_{x\theta} = D\frac{(1-\upsilon)}{2}K_{x\theta}\,.$$

By using Eq. (3-6) and Eq. (3-7) in to Eq. (3-11), the stress and moment resultants can be written in the following form:

$$N_x = \frac{Eh}{1-\upsilon^2}[-\frac{\upsilon w}{R} + \frac{1}{2}(\frac{\partial w}{\partial x})^2 + \frac{\upsilon}{2}(\frac{\partial w}{R\partial\theta})^2 + \frac{\partial u}{\partial x} + \frac{\upsilon}{R}\frac{\partial v}{\partial\theta}]$$

$$N_\theta = \frac{Eh}{1-\upsilon^2}[-\frac{w}{R} + \frac{\upsilon}{2}(\frac{\partial w}{\partial x})^2 + \frac{1}{2}(\frac{\partial w}{R\partial\theta})^2 + \upsilon\frac{\partial u}{\partial x} + \frac{1}{R}\frac{\partial v}{\partial\theta}]$$

$$N_{x\theta} = \frac{Eh}{2(1+\upsilon)}[\frac{w}{R}\frac{\partial u}{\partial\theta} + \frac{1}{R}\frac{\partial w}{\partial x}\frac{\partial w}{\partial\theta} + \frac{\partial v}{\partial x}] \qquad (3\text{-}12)$$

$$M_x = -D(\frac{\partial^2 w}{\partial x^2} + \upsilon\frac{\partial^2 w}{R^2\partial\theta^2})$$

$$M_\theta = -D(\frac{\partial^2 w}{R^2\partial\theta^2} + \upsilon\frac{\partial^2 w}{\partial x^2})$$

$$M_x = -D(1-\upsilon)(\frac{\partial^2 w}{\partial x R\partial\theta})$$

By substituting Eq. (3-6) and Eq. (3-7) in Eq. (3-8) and by using Eq. (3-8) and Eq. (3-10) and substituting Eq. (3-12), the Donnell's governing equations can be obtained as follows:

$$
\begin{aligned}
&RN_{x,x} + N_{x\theta,\theta} = 0\,,\\
&RN_{x\theta,x} + N_{\theta,\theta} = 0\,,\\
&D\nabla^4 w + \frac{1}{R}N_\theta - (N_x w_{,xx} + \frac{2}{R}N_{x\theta}w_{,x\vartheta} + \frac{1}{R^2}N_\theta w_{,\theta\theta}) = 0\,,\\
&\nabla^4 w = (\frac{\partial^2 w}{\partial x^2} + \frac{1}{R^2}\frac{\partial^2 w}{\partial \theta^2})^2\,.
\end{aligned}
\tag{3-13}
$$

Stress resultants in the axial and circumferential directions and the shear resultant are defined based on stress function as follow:

$$
N_x = \frac{1}{R^2}\frac{\partial^2 F}{\partial \theta^2},\ N_\theta = \frac{\partial^2 F}{\partial x^2},\ N_{x\theta} = -\frac{1}{R}\frac{\partial^2 F}{\partial x \partial \theta}.
\tag{3-14}
$$

By substituting Eq. (3-14) in to Eq. (3-13), Donnell's equations of motion will be defined as following and based on Von-Karman theory [63][64][31]:

$$
\begin{aligned}
&D\nabla^4 w + \rho.h.\ddot{w} = \frac{1}{R}\frac{\partial^2 F}{\partial x^2} + (\frac{1}{R^2}\frac{\partial^2 F}{\partial \theta^2}w_{,xx} - \frac{2}{R^2}\frac{\partial^2 F}{\partial x.\partial \theta}w_{,x\vartheta} + \frac{1}{R^2}\frac{\partial^2 F}{\partial x^2}w_{,\theta\theta})\,,\\
&\frac{1}{E.h}\nabla^4 F = -\frac{1}{R}\frac{\partial^2 w}{\partial x^2} - \frac{\partial^2 w}{\partial x^2}.\frac{\partial^2 w}{\partial \theta^2} + (\frac{\partial^2 w}{\partial x.\partial \theta})^2\,,
\end{aligned}
\tag{3-15}
$$

$$\nabla^4 w = (\frac{\partial^2 w}{\partial x^2} + \frac{1}{R^2}\frac{\partial^2 w}{\partial \theta^2})^2 .$$

Where F is the in-plane Airy stress, dot stands for the derivative respect to time t and ρ is mass density of shell.

3.2. The Nonlocal Elastic Shell Model

The nonlocal theory has been explained completely in the chapter. 2. Following Eringen's elasticity theory and using Eq. (2-2), the nonlocal stress–strain relationships is in the following form [19]:

$$\begin{aligned}
&\sigma_x - (e_0 a)^2 \nabla^2 \sigma_x = \frac{E}{(1-\upsilon^2)}(\varepsilon_x + \upsilon \varepsilon_\theta), \\
&\sigma_\theta - (e_0 a)^2 \nabla^2 \sigma_\theta = \frac{E}{(1-\upsilon^2)}(\varepsilon_\theta + \upsilon \varepsilon_x) \\
&\tau_{x\theta} - (e_0 a)^2 \nabla^2 \tau_{x\theta} = \frac{E}{2(1+\upsilon)}\gamma_{x\theta}
\end{aligned} \tag{3-16}$$

Based on Eq. (3-16), force and moment resultants in the nonlocal form can be written as [65]:

$$N_x = C(\varepsilon_x + \upsilon \varepsilon_\theta) + (e_0 a)^2 \nabla^2 N_x$$

$$N_\theta = C(\varepsilon_\theta + \upsilon \varepsilon_x) + (e_0 a)^2 \nabla^2 N_\theta$$

$$N_{x\theta} = C\frac{(1-\upsilon)}{2}\gamma_{x\theta} + (e_0 a)^2 \nabla^2 N_{x\theta} \tag{3-17}$$

$$M_x = D(k_x + \upsilon k_\theta) + (e_0 a)^2 \nabla^2 M_x$$

$$M_\theta = D(k_\theta + \upsilon k_x) + (e_0 a)^2 \nabla^2 M_\theta$$

$$M_{x\theta} = D\frac{(1-\upsilon)}{2}K_{x\theta} + (e_0 a)^2 \nabla^2 M_{x\theta}$$

By using Eq. (3-6) and Eq. (3-7) in to Eq. (3-17), the stress and moment resultants can be written in the following form:

$$N_x - (e_0 a)^2 \nabla^2 N_x = \frac{Eh}{1-\upsilon^2}[-\frac{\upsilon w}{R} + \frac{1}{2}(\frac{\partial w}{\partial x})^2 + \frac{\upsilon}{2}(\frac{\partial w}{R\partial \theta})^2 + \frac{\partial u}{\partial x} + \frac{\upsilon}{R}\frac{\partial v}{\partial \theta}]$$

$$N_\theta - (e_0 a)^2 \nabla^2 N_\theta = \frac{Eh}{1-\upsilon^2}[-\frac{w}{R} + \frac{\upsilon}{2}(\frac{\partial w}{\partial x})^2 + \frac{1}{2}(\frac{\partial w}{R\partial \theta})^2 + \upsilon\frac{\partial u}{\partial x} + \frac{1}{R}\frac{\partial v}{\partial \theta}]$$

$$N_{x\theta} - (e_0 a)^2 \nabla^2 N_{x\theta} = \frac{Eh}{2(1+\upsilon)}[\frac{w}{R}\frac{\partial u}{\partial \theta} + \frac{1}{R}\frac{\partial w}{\partial x}\frac{\partial w}{\partial \theta} + \frac{\partial v}{\partial x}] \tag{3-18}$$

$$M_x - (e_0 a)^2 \nabla^2 M_x = -D(\frac{\partial^2 w}{\partial x^2} + \upsilon\frac{\partial^2 w}{R^2 \partial \theta^2})$$

$$M_\theta - (e_0 a)^2 \nabla^2 M_\theta = -D(\frac{\partial^2 w}{R^2 \partial \theta^2} + \upsilon\frac{\partial^2 w}{\partial x^2})$$

$$M_{x\theta} - (e_0 a)^2 \nabla^2 M_{x\theta} = -D(1-\upsilon)(\frac{\partial^2 w}{\partial x R \partial \theta})$$

By using Eq. (3-8) and Eq. (3-10) and substituting Eq. (3-18), the Donnell's governing equations based on nonlocal elasticity can be obtained as follows:

$$\frac{\partial N_x}{\partial x}+(e_0a)^2\frac{\partial}{\partial x}\nabla^2 N_x+\frac{1}{R}\frac{\partial N_{x\theta}}{\partial \theta}+\frac{1}{R}(e_0a)^2\frac{\partial}{\partial \theta}\nabla^2 N_{x\theta}=\rho h\ddot{u},$$

$$\frac{\partial N_{x\theta}}{\partial x}+(e_0a)^2\frac{\partial}{\partial x}\nabla^2 N_x+\frac{1}{R}\frac{\partial N_{\theta}}{\partial \theta}+\frac{1}{R}(e_0a)^2\frac{\partial}{\partial \theta}\nabla^2 N_{\theta}=\rho h\ddot{v}, \tag{3-19}$$

$$\frac{\partial^2 M_x}{\partial x^2}+(e_0a)^2\frac{\partial^2}{\partial x^2}\nabla^2 M_x+\frac{2}{R}(\frac{\partial^2 M_{x\theta}}{\partial x\partial \theta}+(e_0a)^2\frac{\partial^2}{\partial x\partial \theta}\nabla^2 M_{x\theta})+\frac{1}{R^2}(\frac{\partial^2 M_{\theta}}{\partial \theta^2}+$$
$$(e_0a)^2\frac{\partial^2}{\partial \theta^2}\nabla^2 M_{\theta})-\frac{1}{R}(N_{\theta}+(e_0a)^2\nabla^2 N_{\theta})+[(N_x+(e_0a)^2\nabla^2 N_x)w,_{xx}+$$
$$\frac{2}{R}(N_{x\theta}+(e_0a)^2\nabla^2 N_{x\theta})$$
$$w,_{x\theta}+\frac{1}{R^2}(N_{\theta}+(e_0a)^2\nabla^2 w,_{\theta\theta}]=\rho h\ddot{w}$$

In Donnell's nonlinear theory, only nonlinear terms that depend on w are maintained and all other nonlinear terms are ignored. Therefore, the third equation of motion will be changed to:

$$\frac{\partial^2 M_x}{\partial x^2}+\frac{2}{R}\frac{\partial^2 M_{x\theta}}{\partial x\partial \theta}+\frac{1}{R^2}\frac{\partial^2 M_{\theta}}{\partial \theta^2}-\frac{N_{\theta}}{R}+[N_x w,_{xx}+\frac{2}{R}N_{x\theta}w,_{x\theta}+\frac{1}{R^2}N_{\theta}w,_{\theta\theta}]= \tag{3-20}$$
$$\rho h\ddot{w}-\rho h(e_0a)^2(\ddot{w}_{xx}+\frac{1}{R^2}\ddot{w}_{\theta\theta})$$

By substituting Eq. (3-14) in to Eq. (3-20), Donnell's equations of motion based on nonlocal theory will be defined as follow:

$$D\nabla^4 w + \rho h\ddot{w} - \rho h(e_0 a)^2(\ddot{w}_{xx} + \frac{\ddot{w}_{\theta\theta}}{R^2}) = \frac{1}{R}\frac{\partial^2 w}{\partial x^2} + \frac{1}{R^2}(\frac{\partial^2 F}{\partial \theta^2}\frac{\partial^2 w}{\partial x^2} - 2\frac{\partial^2 F}{\partial x \partial \theta}\frac{\partial^2 w}{\partial x \partial \theta} + \frac{\partial^2 F}{\partial x^2}\frac{\partial^2 w}{\partial \theta^2}) \quad (3\text{-}21\text{-a})$$

$$\nabla^4 w = (\frac{\partial^2 w}{\partial x^2} + \frac{1}{R^2}\frac{\partial^2 w}{\partial \theta^2})^2$$

$$\nabla^4 F - (e_0 a)^2(\nabla^6 F) = EH(-\frac{1}{R}\frac{\partial^2 w}{\partial x^2} + \left[\left(\frac{\partial^2 w}{R\partial x \partial \theta}\right)^2 - \frac{\partial^2 w}{\partial x^2}\frac{\partial^2 w}{R^2 \partial \theta^2}\right] \quad (3\text{-}21\text{-b})$$

$$\nabla^6 w = (\frac{\partial^2 w}{\partial x^2} + \frac{1}{R^2}\frac{\partial^2 w}{\partial \theta^2})^3$$

In this study, the attention is focused on a finite, simply supported ends circular cylindrical shell with length L. The following boundary conditions are defined as:

$$v = w = 0, N_x = 0, M_x = 0, x = 0, L \quad (3\text{-}22)$$

3.3. Solution Procedure

For solving the nonlinear Donnell's equation, the shape mode for radial displacement and for continuum shell based on the simple boundary condition is defined as follow [66][17]:

$$w(x,\theta,t) = A(t)\cos(n\theta)\sin(\frac{m\pi x}{L}) + \frac{n^2}{4R}A(t)^2\sin(\frac{m\pi x}{L})^2. \quad (3\text{-}23)$$

Where m is the axial wave number and equal to the number of half-waves along the shell, and n is the circumferential wave number. A(t) is the amplitude function and it is an unknown generalized time function of the vibration.

By substituting Eq. (3-23) in the right-hand side of Eq. (3-21-b) and solving for the particular solution lead to:

$$F = Eh(A_1\cos(2n\theta) + A_2\cos(n\theta)\sin(\frac{3m\pi x}{L}) + A_3\cos(n\theta)\sin(\frac{m\pi x}{L})) \quad (3\text{-}24)$$

Where A_1, A_2 and A_3 are not reported here for the sake of brevity and can be found in Appendix A.1.

By substituting Eq. (3-23) and Eq. (3-24) in Eq. (3-21-a), there is a complicated partial differential equation (PDE) which cannot be solved by the separation of variables. Therefore, it is necessary to use the numerical method for changing this PDE to ordinary differential equation (ODE). In this thesis, Galerkin method will be used.

3.3.1. Galerkin Method

Galerkin method is one of the finite element methods for solving the nonlinear partial differential of the equation which employs basis function φ_i and approximates the nonlinear partial differential of equations (PDEs) and transformed it to finite coupled ordinary differential of equations (ODEs) [59]. The overall picture of this method for a differential of the equation is as follow:

$$\left(D\nabla^4 w + \rho h \ddot{w} = ..., \varphi \right) = \int_0^{2\pi} \int_0^{l} (D\nabla^4 w + \rho h \ddot{w} = ...) \times \varphi \tag{3-25}$$

Where φ_i is Galerkin weight function which is obtained by the first derivation of Eq. (3-23) respect to A(t) and is defined as:

$$\varphi = \cos(n\theta)\sin(\frac{m\pi x}{L}) + \frac{n^2}{2R} A(t)\sin(\frac{m\pi x}{L})^2 \tag{3-26}$$

By using the Galerkin method, nonlinear PDE is changed to below ODE:

$$\begin{aligned} &\gamma_1 A(t) + \gamma_2 A(t)^3 + \gamma_3 A(t)^2 (\frac{d^2}{dt^2} A(t)) + \gamma_4 A(t)(\frac{d^2}{dt^2} A(t)) + \gamma_5 A(t)(\frac{d}{dt} A(t))^2 + \\ &\gamma_6 (\frac{d}{dt} A(t))^2 + (e_0 a)^2 \gamma_7 A(t)^2 (\frac{d^2}{dt^2} A(t)) + (e_0 a)^2 \gamma_8 A(t)(\frac{d}{dt} A(t))^2 + \\ &(e_0 a)^2 \gamma_9 (\frac{d^2}{dt^2} A(t)) = \begin{bmatrix} \gamma_{10} A(t)^3 + \gamma_{11} A(t) + \gamma_{12} A(t)^5 + (e_0 a)^2 \gamma_{13} A(t)^3 \\ + (e_0 a)^4 \gamma_{14} A(t)^3 + (e_0 a)^4 \gamma_{15} A(t)^5 + (e_0 a)^4 \gamma_{16} A(t) \end{bmatrix} / \\ &\left[\gamma_{17} + (e_0 a)^2 \gamma_{18} + (e_0 a)^4 \gamma_{19} \right] \end{aligned} \tag{3-27}$$

γ values are reported in Appendix A.2.

Since the above mentioned equation is nonlinear, it is impossible to solve it completely. Therefore, we are going to use the averaging method to solve the above ODE approximately.

3.3.2. Averaging Method

Averaging method is one of the perturbation methods for solving the nonlinear equations analytically. Based on the averaging method, the solution is written as:

$$A(t) = a(t)\cos(\omega t + \beta(t)) \tag{3-28}$$

Where $a(t)$ and $\beta(t)$ are functions of t (time). The first derivation of Eq. (3-28) by considering $a(t), \beta(t)$ are constant is defined as:

$$\dot{A}(t) = -a(t)\omega\sin(\omega t + \beta(t)), \tag{3-29}$$

For determining the equations describing $a(t)$ and $\beta(t)$, we differentiate Eq. (3-28) respect to t and obtain:

$$\dot{A}(t) = -a(t).\omega.\sin(\omega t + \beta(t)) + \dot{a}(t).\cos(\omega t + \beta(t)) - a.\dot{\beta}(t).\sin(\omega t + \beta(t)) \tag{3-30}$$

With comparing Eq.(3-28) and Eq. (3-29), the below equation is obtained:

$$\dot{a}(t).\cos(\omega t + \beta(t)) - a.\dot{\beta}(t).\sin(\omega t + \beta(t)) = 0 \tag{3-31}$$

The second derivation of Eq. (3-27) is defined as:

$$\ddot{A}(t) = -a(t)\omega^2 \cos(\omega t + \beta(t)) - \dot{a}(t)\omega \sin(\omega t + \beta(t)) - a(t)\dot{\beta}(t)\cos(\omega t + \beta(t)). \quad (3\text{-}32)$$

Finally, we have following equations:

$$\begin{aligned} A(t) &= a(t)\cos(wt + \beta(t)), \\ \dot{A}(t) &= -a(t)\omega \sin(\omega t + \beta(t)), \\ \ddot{A}(t) &= -a(t)\omega^2 \cos(\omega t + \beta(t)) - \dot{a}(t)\omega \sin(\omega t + \beta(t)) - a(t)\dot{\beta}(t)\cos(\omega t + \beta(t)). \end{aligned} \quad (3\text{-}33)$$

The above-mentioned equations are substituted to Eq. (3-27) and by integrating in one period of vibration, and assuming that $a(t)$ and $\beta(t)$ hardly changes with time, Eq. (3-27) will be averaged and solved. On the other hand, in this study the steady state response has been considered which means that the average value of $a(t)$ and $\beta(t)$ remain steady with time [67]. Hence, the average of $\dot{\beta}(t)$ is identically zero. Then Eq. (3-27) is reduced as:

$$\begin{aligned} &\overline{\alpha}_1 a(t) + \overline{\alpha}_2 a(t)^3 + \overline{\alpha}_3 a(t)^3 \omega^2 + \overline{\alpha}_4 a(t)\omega^2 + (e_0 a)^2 \overline{\alpha}_5 a(t)^3 \omega^2 + (e_0 a)^2 \overline{\alpha}_5 a(t)\omega^2 = \\ &\left[\begin{array}{l} \overline{\alpha}_7 a(t)^3 + \overline{\alpha}_8 a(t) + \overline{\alpha}_9 a(t)^5 + (e_0 a)^2 \overline{\alpha}_{10} a(t) + (e_0 a)^4 \overline{\alpha}_{11} a(t) + (e_0 a)^2 \overline{\alpha}_{12} a(t)^3 + \\ (e_0 a)^2 \overline{\alpha}_{13} a(t)^5 + (e_0 a)^4 \overline{\alpha}_{14} a(t)^3 + (e_0 a)^4 \overline{\alpha}_{15} a(t)^5 \end{array} \right] / \\ &\left[\overline{\alpha}_{16} + (e_0 a)^2 \overline{\alpha}_{17} + (e_0 a)^4 \overline{\alpha}_{18} + (e_0 a)^6 \overline{\alpha}_{19} \right] \end{aligned} \quad (3\text{-}34)$$

$\overline{\alpha}$ values are reported in Appendix A.3.

3.3.3. Non-dimensionless Variables

For solving Eq. (3-34) and obtaining the nonlinear frequency, the non-dimensionless variables are defined as follow:

$$\overline{A} \equiv \frac{A}{h},$$

$$F_{Linear}{}^{2} = \frac{E}{\rho R^{2} + \overline{\mu}^{2}(\xi^{2}+1)}\left[\frac{\xi^{4}}{(\xi^{2}+1)^{2} + \overline{\mu}^{2}(\xi^{2}+1)^{3}} + \frac{\varepsilon(\xi^{2}+1)^{2}}{12(1-\upsilon^{2})}\right], \tag{3-35}$$

$$\Omega = \frac{\omega}{F_{Linear}}$$

$$\overline{\mu} = \frac{(e_0 a)\times n}{R},\ \xi = \frac{m\pi R}{nl},\ \varepsilon = (\frac{n^2 h}{R})^2$$

Where $\overline{A}$ is non-dimensionless amplitude, F_{Linear} is linear frequency[43], $\overline{\mu}$ is a non-dimensionless nonlocal parameter, ξ is aspect ratio, ε is a nonlinear parameter and Ω is the ratio of the nonlinear frequency to the linear frequency called non-dimensionless frequency either. With substituting the above parameters in Eq. (3-34), a non-dimensionless form of the equation is defined as:

$$-\Omega^{2}((1+\overline{\mu}^{2}b_1)\overline{A} + b_2\overline{A}^{3}) + b_3\overline{A} + b_4\overline{A}^{3} + b_5\overline{A}^{5} = o. \tag{3-36}$$

b values are reported in Appendix A.4.

3.4. Results Verification

The results of this study have been verified with the results which Evensen [66] had obtained for the macro shell. When the nonlocal parameter is equal to zero ($e_0 a = 0$), the nonlinear equation reduces to equations reported by Evensen [66] and the results are the same.

3.5. Numerical Results and Discussion

For investigation nonlinear dynamic behavior of SWCNT, three various zigzag SWCNT (10,0), (20,0) and (30,0) have been selected which the corresponding geometries have been reported by Gupta[68] which are shown in the table. (2).

Maple software has been used for derivation of the equations of motion, Galerkin's method and averaging method. Then, the related graphs have been plotted by using MATLAB software.

The effects of various parameters (nonlocal parameters, nonlinear parameters, aspect ratios and wave numbers) on the nonlinear dynamic behavior of an ideal SWCNT are studied based on the nonlocal elasticity theory. Moreover, the difference between classical and nonlocal theories is studied in this part.

Table 3-1: Results Verification

ξ	ε	Ω **(Ref.[66])**	Ω **Present Study with** $e_0 a = 0nm$
1/4	0	1	1
	0.1	0.753402	0.753402
	1	0.841588	0.841588
2	0	1	1
	0.1	1.34189	1.34189
	1	2.26765	2.26765

Table 3-2: Geometries of SWCNT [68]

Tube (p , q)	υ	**Radius** $R(\overset{\circ}{A})$	$h(\overset{\circ}{A})$	$E(Tpa)$	$D(eV)$
(10,0)	0.265	3.713	0.878	3.939	1.389
(20,0)	0.238	7.420	1.251	2.704	2.811
(30,0)	0.227	11.129	1.340	2.493	3.244

3.5.1. Effects of Small -Scale on the Nonlinear Dynamic of SWCNT

The effects of small-scale (various nonlocal parameters) on the nonlinear dynamic behavior of SWCNT have been shown in the figure 3-2 to figure 3-5. A (10,0) zigzag SWCNT has been chosen with nonlinear parameter equal to $\varepsilon = 0.0559$ and the wave numbers are *m=n=1*. Figure 3-2 shows the effect of nonlocal parameters on the nonlinear dynamic behavior of an SWCNT and compared it with the classical theory. The aspect ratios are considered $\xi = 0.25$ and $\xi = 4$. It is seen that by using the nonlocal elasticity theory, nonlinearity reduces in the system. Moreover, it is observed that difference between two theories falls by using the longer CNTs (smaller aspect ratios). It means for the long CNTs; it is possible to use the classical theories with a good approximation. Also, it is seen that nonlinear behavior is softening type at the lower amplitudes which changes to hardening type at the higher amplitude for the long CNT .However; it is the hardening type for the short CNT $\xi = 4$ at any amplitudes. Figure 3-3 represents the influence of the nonlocal parameter on the vibration amplitude of short CNT and it shows that increasing the nonlocal parameter decreases the hardening behavior. Figure 3-4 and figure 3-5 plotted to show the effect of the nonlocal parameter on the vibration amplitudes for the long CNT at the lower and the higher amplitudes respectively. The figures reveal that raising the nonlocal parameter causes an increment in the softening behavior at the lower amplitude, and it decreases the hardening behavior at the higher amplitudes.

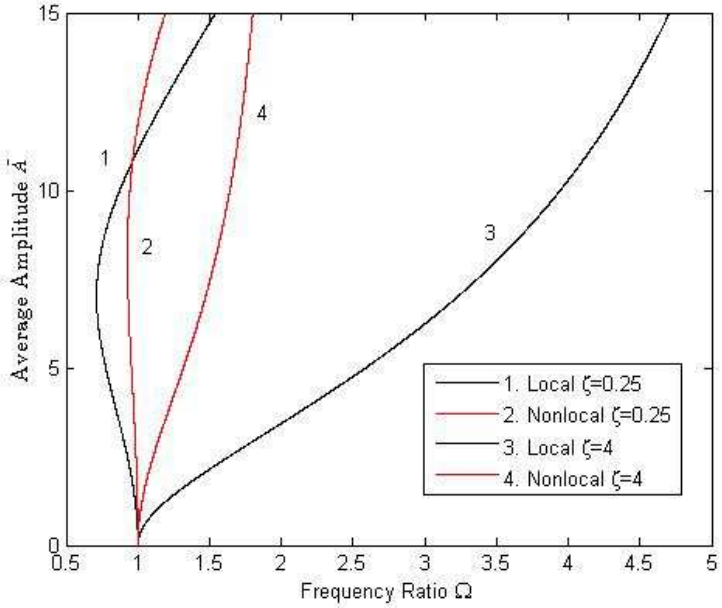

Figure 3-2: Comparison between classical and nonlocal theory.

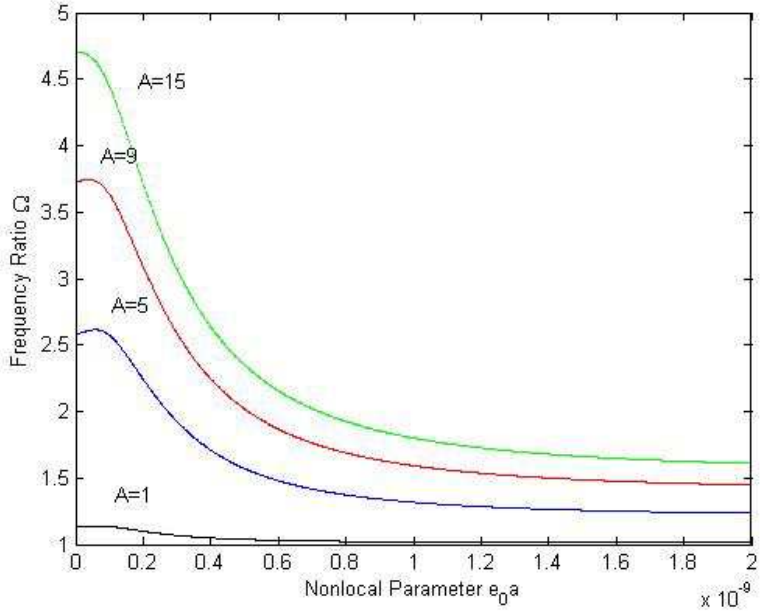

Figure 3-3: Effect of small-scale on the vibration amplitude for $\xi = 4$

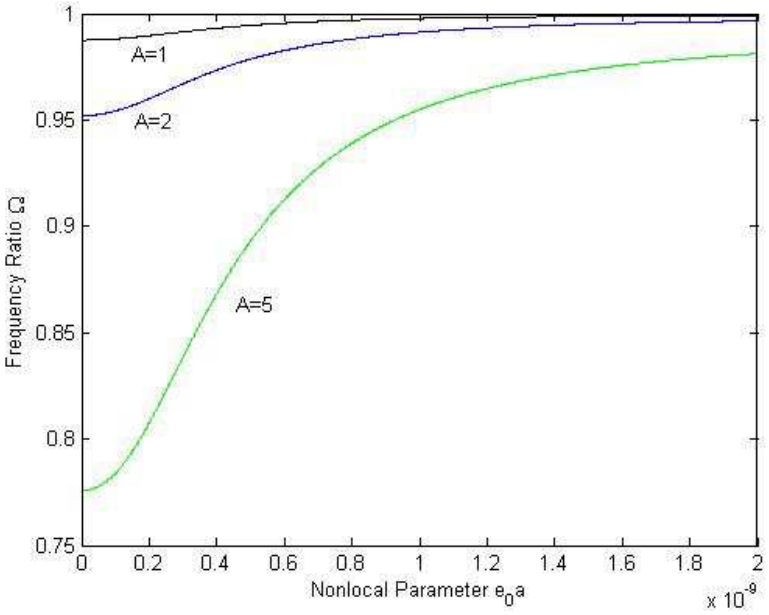

Figure 3-4: Effect of small-scale on the lower vibration amplitude for $.\xi = 0.25$

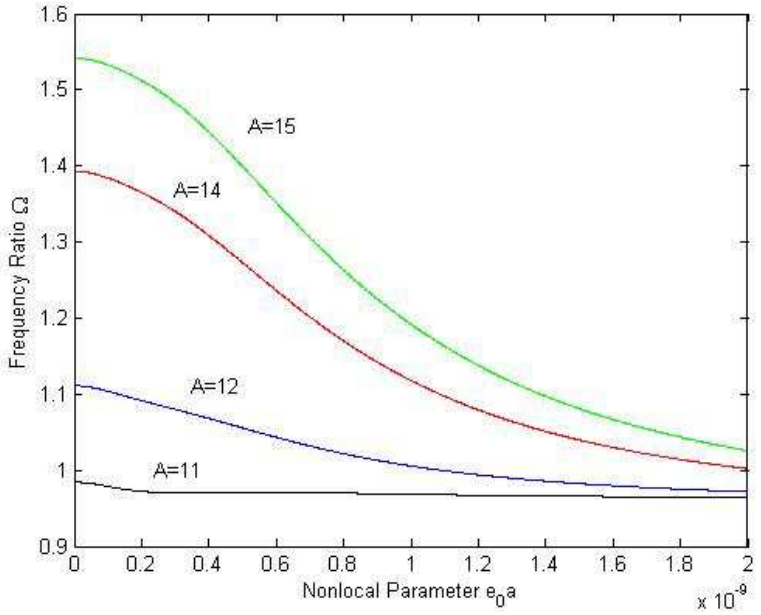

Figure 3-5: Effect of small-scale on the higher vibration amplitude for $.\xi = 0.25$

3.5.2. Effects of Different Nonlinear Parameters on the Nonlinear Dynamic of SWCNT based on both Theories

Effects of various nonlinear parameters have been shown in figure 3-6. The nonlinear parameters are: $\varepsilon = 0.0559$ $\varepsilon = 0.0248$ and $\varepsilon = 0.0145$ the aspect ratio is $\xi = 0.25$ and wave numbers are *m=1* and *n=1*. The nonlocal parameter is equal to $e_0 a = 1nm$. For obtaining the various nonlinear parameters, three different zigzag SWCNTs have been selected. It is seen that nonlinear vibration behavior is increased by increasing the nonlinear parameters. However, it is observed that by using the nonlocal elasticity theory, nonlinearity is reduced for all three types SWCNTs. Also, it is seen that changing the softening behavior to the hardening type occurs at the larger amplitude by using the nonlocal theory.

3.5.3. Effects of Different Aspect Ratios on the Nonlinear Dynamic of SWCNT based on nonlocal elasticity theory

The effects of various aspect ratios for (10,0) zigzag SWCNT have been shown in the figure 3-7. The wave numbers are *m=1* and *n=1* and the aspect ratios are $\xi = 0.25$ & 0.5 (long CNTs) and are $\xi = 2$ & 4 (short CNTs). It is seen that nonlinear frequency is increased by increment the aspect ratios. Moreover, it is observed that nonlinear dynamic behavior for the long CNTs is softening type at the lower amplitude which is changed to hardening type at the higher amplitude. However, nonlinear dynamic behavior for the short CNTs is just hardening type.

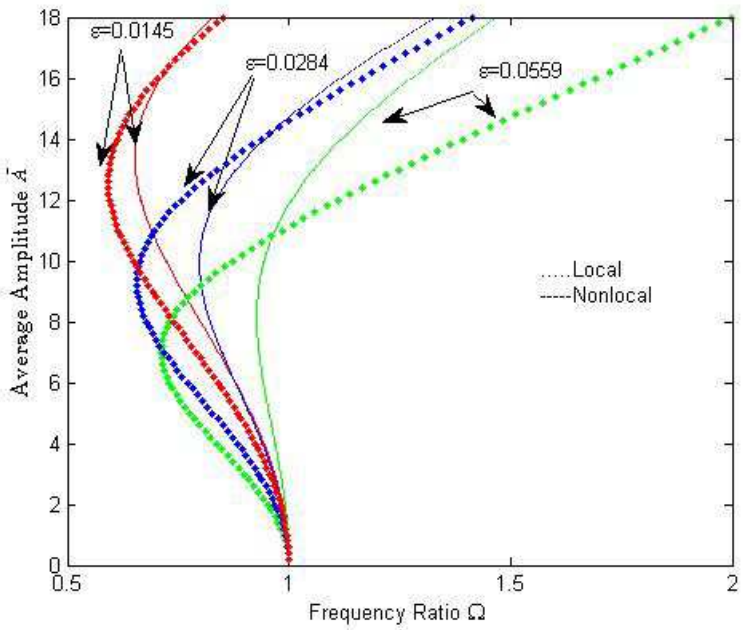

Figure 3-6: Effects of various nonlinear parameters on nonlinear dynamic behavior of CNTs

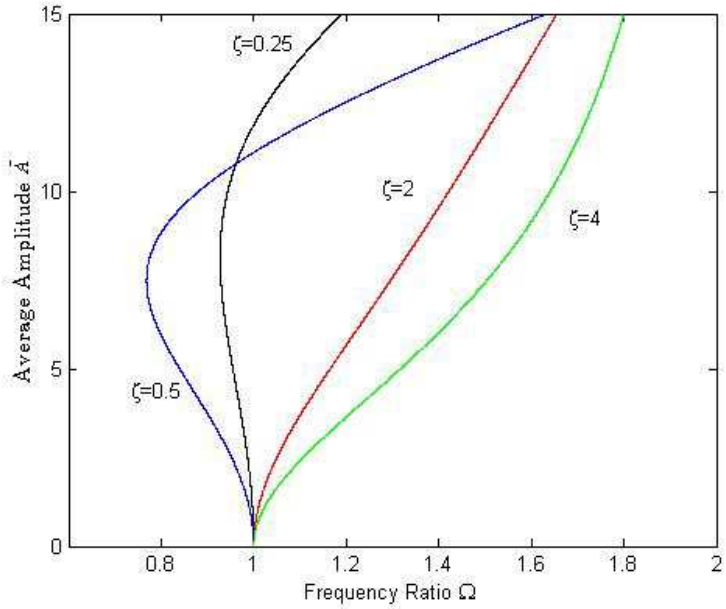

Figure 3-7: Effect of various aspect ratios on nonlinear dynamic behavior of SWCNT based on nonlocal elasticity theory.

3.5.4. Effect of Different Wave Numbers on the Nonlinear Dynamic of SWCNT based on Nonlocal Elasticity Theory

Figure 3-8 reveals an influence of diverse wave numbers on the nonlinear vibration of (10,0) zigzag SWCNT. Since circumferential wave number has the most effect on the various non-dimensional parameters (ε, ξ and μ), therefore the effect of circumferential wave numbers is studied in this part. The length of CNT has been considered $l = 4\pi R$ and the nonlocal parameter is $e_0 a = 1nm$. Increment the circumferential wave number increases the nonlinear parameter and decreases the aspect ratio, and finally makes more nonlinearity in vibration behavior and increases the softening behavior. Also, it is seen that changing the softening behavior to the hardening type occurs at the higher amplitudes.

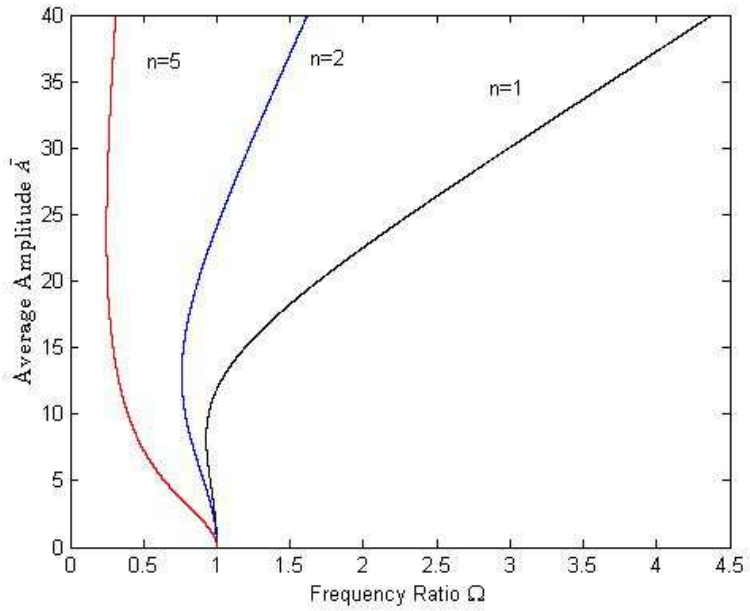

Figure 3-8: Effect of various wave numbers on nonlinear dynamic behavior of CNT based on nonlocal elasticity theory

4 Chapter Four: Nonlinear Dynamic Analysis of SWCNT with an Initial Geometric Imperfection

The impact of an initial geometric imperfection on the nonlinear dynamic behavior of SWCNT has been considered in this chapter. This chapter is divided in to two sections. In the first part an imperfect SWCNT was modeled based on the classical shell theory and in the second part an imperfect SWCNT was modeled based on nonlocal shell theory and the effect of various parameters on the frequency of SWCNT have been studied and compared with the classical theory. The effects of imperfection, different nonlinear parameters, and the various aspect ratios on the nonlinear dynamic behavior of SWCNT have been discussed in detail.

4.1. The Effects of Imperfection on the Nonlinear Dynamic Behavior of SWCNT based on Classical (Local) Theory

4.1.1. Modeling of SWCNT with an Initial Geometric Imperfection

Based on the explanations in the previous chapter, w is the radial displacement from the middle surface of the shell. An initial geometric imperfection is defined by w_0 which measured from the middle surface of the shell. Therefore, the small rotation angles w_x and w_θ is replaced by $(w+w_0)_x$ and $(w+w_0)_\theta$ for the SWCNT with an initial geometric imperfection [17][59].

Based on chapter three, the strain components $\bar{\varepsilon}_x, \bar{\varepsilon}_\theta$ and $\bar{\gamma}_{x\theta}$ are at arbitrary points of shell related to the middle surface strains $\varepsilon_x, \varepsilon_\theta$ and $\gamma_{x\theta}$ as well as the changes in the curvature and torsion of the middle surface k_x, k_θ and $k_{x\theta}$

$$\bar{\varepsilon}_x = \varepsilon_x + zk_x,$$

$$\bar{\varepsilon}_\theta = \varepsilon_\theta + zk_\theta, \tag{4-1}$$

$$\bar{\gamma}_{x\theta} = \gamma_{x\theta} + zk_{x\theta}.$$

Strain components at the middle surface of shell considering the initial geometric imperfection are defined as:

$$\varepsilon_x = \frac{\partial u}{\partial x} + \frac{1}{2}(\frac{\partial w}{\partial x})^2 + \frac{\partial w}{\partial x}\frac{\partial w_0}{\partial x},$$

$$\varepsilon_\theta = \frac{1}{R}\frac{\partial v}{\partial \theta} + \frac{w}{R} + \frac{1}{2R^2}(\frac{\partial w}{\partial \theta})^2 + \frac{\partial w}{R\partial \theta}\frac{\partial w_0}{R\partial \theta}, \tag{4-2}$$

$$\gamma_{x\theta} = \frac{1}{R}\frac{\partial u}{\partial \theta} + \frac{\partial v}{\partial x} + \frac{1}{R}(\frac{\partial w}{\partial \theta})(\frac{\partial w}{\partial x}) + \frac{\partial w}{\partial x}\frac{\partial w_0}{R\partial \theta} + \frac{\partial w_0}{\partial x}\frac{\partial w}{R\partial \theta}.$$

And the curvatures of the middle surface are:

$$k_x = -\frac{\partial^2 w}{\partial x^2},$$

$$k_\theta = -\frac{\partial^2 w}{R^2 \partial \theta^2}, \tag{4-3}$$

$$k_{x\theta} = -\frac{2}{R}\frac{\partial^2 w}{\partial \theta \partial x}.$$

Based on the initial imperfection, the stress resultants are written as:

$$N_x = \frac{EH}{1-\upsilon^2}[-\frac{\upsilon w}{R}+\frac{1}{2}(\frac{\partial w}{\partial x})^2+\frac{\partial w}{\partial x}\frac{\partial w_0}{\partial x}+\frac{\upsilon}{2}(\frac{\partial w}{R\partial\theta})^2+\upsilon\frac{\partial w}{R\partial\theta}\frac{\partial w_0}{R\partial\theta}+\frac{\partial u}{\partial x}+\frac{\upsilon}{R}\frac{\partial \upsilon}{\partial\theta}],$$

$$N_\theta = \frac{EH}{1-\upsilon^2}[-\frac{w}{R}+\frac{\nu}{2}(\frac{\partial w}{\partial x})^2+\nu\frac{\partial w}{\partial x}\frac{\partial w_0}{\partial x}+\frac{1}{2}(\frac{\partial w}{R\partial\theta})^2+\upsilon\frac{\partial u}{\partial x}+\frac{\partial w}{R\partial\theta}\frac{\partial w_0}{R\partial\theta}+\frac{1}{R}\frac{\partial \upsilon}{\partial\theta}], \quad (4\text{-}4)$$

$$N_{x\theta} = \frac{EH}{2(1+\upsilon)}[\frac{1}{R}\frac{\partial u}{\partial\theta}+\frac{\partial w}{\partial x}\frac{\partial w_0}{R\partial\theta}+\frac{\partial w_0}{\partial x}\frac{\partial w}{R\partial\theta}+\frac{1}{R}\frac{\partial w}{\partial x}\frac{\partial w}{\partial\theta}+\frac{\partial \upsilon}{\partial x}].$$

The Donnell's equations of motion for the SWCNT with an initial geometric imperfection are derived based on the explanations in chapter three and the aforementioned new components:

$$D\nabla^4 w-\frac{1}{R}\frac{\partial^2 F}{\partial x^2}-(\frac{\partial^2 F}{R^2\partial\theta^2}(w_{,xx}+w_{0,xx})-\frac{2}{R^2}\frac{\partial^2 F}{\partial x\partial\theta}(w_{,x\vartheta}+w_{0,x\vartheta})+ \quad (4\text{-}5\text{-a})$$
$$\frac{1}{R^2}\frac{\partial^2 F}{\partial x^2}(w_{,\theta\theta}+w_{0,\theta\theta})=-\rho h\ddot{w}$$

$$\nabla^4 F = EH(-\frac{1}{R}\frac{\partial^2 w}{\partial x^2}+\frac{1}{R^2}\begin{pmatrix}(\frac{\partial^2 w}{\partial x\partial\theta})^2+2\frac{\partial^2 w}{\partial x\partial\theta}\frac{\partial^2 w_0}{\partial x\partial\theta}-(\frac{\partial^2 w}{\partial x^2}+\frac{\partial^2 w_0}{\partial x^2})\frac{\partial^2 w}{\partial\theta^2}\\ -\frac{\partial^2 w}{\partial x^2}\frac{\partial^2 w_0}{\partial\theta^2}\end{pmatrix}) \quad (4\text{-}5\text{-b})$$

$$\nabla^4 w=(\frac{\partial^2 w}{\partial x^2}+\frac{1}{R^2}\frac{\partial^2 w}{\partial\theta^2})^2$$

Where F is the in-plane Airy Stress and the stress resultants in the axial and circumferential directions, and the shear resultant are defined based on stress function as follow:

$$N_x = \frac{1}{R^2}\frac{\partial^2 F}{\partial \theta^2},$$

$$N_\theta = \frac{\partial^2 F}{\partial x^2}, \tag{4-7}$$

$$N_{x\theta} = -\frac{1}{R}\frac{\partial^2 F}{\partial x \partial \theta}.$$

4.1.2. Solution Procedure

For solving the nonlinear Donnell's equation with an initial imperfection, the shape mode for radial displacement based on the simple boundary condition is defined as follow [66][17]:

$$w(x,\theta,t) = A(t)\cos(n\theta)\sin(\frac{m\pi x}{L}) + \frac{n^2}{4R}A(t)^2\sin(\frac{m\pi x}{L})^2. \tag{4-8}$$

Based on comprehensive explanation about imperfection in chapter one, a widespread imperfection is a wide variety of defects including defects and combinations of them. SWCNT has been modeled the same as the cylindrical shell with an initial geometric imperfection. This initial imperfection has been considered as a simple model which represents the widespread defects on the carbon nanotube.

$$w_0(x,\theta) = W_0\sin(n\theta)\sin(\frac{m\pi x}{L}) \tag{4-9}$$

This model has been by far in various studies [17].

By substituting Eq. (4-8) and Eq. (4-9) in the right-hand side of Eq. (4-5-b) and solving it the particular solution is:

$$F_p = A_1 \sin(n\theta)\sin(\frac{3m\pi x}{L}) + A_2 \cos(n\theta)\sin(\frac{3m\pi x}{L}) + A_3 \sin(n\theta)\sin(\frac{m\pi x}{L}) + \\ A_4 \cos(n\theta)\sin(\frac{m\pi x}{L}) + + A_5 \cos(2n\theta) + A_6 \sin(2n\theta) \quad (4\text{-}10)$$

Where A values are not reported here for the sake of brevity and can be found in Appendix B.1.

By substituting Eq. (4-8), Eq. (4-9) and Eq. (4-10) in Eq. (4-5-a), there is a complicated partial differential equation (PDE) which cannot be solved by the separation of variables. Therefore, it is necessary to use the numerical method for changing this PDE to ordinary differential equation (ODE). In this thesis, Galerkin method will be used.

Similar to the solution procedure described in part (3.3) and by using the Galerkin method, the PDE is changed to following ODE:

$$\tilde{\alpha}_1 A(t)^3 + \tilde{\alpha}_2 A(t) + \tilde{\alpha}_3 (\frac{d}{dt} A(t))^2 A(t) + \tilde{\alpha}_4 (\frac{d^2}{dt^2} A(t)) A(t)^2 + \tilde{\alpha}_5 (\frac{d^2}{dt^2} A(t)) = \\ (\tilde{\alpha}_6 A(t)^3 + \tilde{\alpha}_7 w^2 + \tilde{\alpha}_8 A(t)^5 + \tilde{\alpha}_9 A(t)) \quad (4\text{-}11)$$

$\tilde{\alpha}$ values are reported in Appendix B.2.

Above mentioned equation is nonlinear, and it is impossible to solve it directly. Therefore, averaging method is used to solve the above ODE approximately.

$$\overline{\overline{\alpha}}_1 A + \overline{\overline{\alpha}}_2 A^3 \omega^2 + \overline{\overline{\alpha}}_3 A^3 + \overline{\overline{\alpha}}_4 A \omega^2 = \overline{\overline{\alpha}}_5 A^3 W_0^{\ 2} + \overline{\overline{\alpha}}_6 A^3 + \overline{\overline{\alpha}}_7 A^5 + \overline{\overline{\alpha}}_8 A W_0^{\ 2} + \overline{\overline{\alpha}}_9 A \qquad (4\text{-}12)$$

$\overline{\overline{\alpha}}$ values are reported in Appendix B.3.

For solving Eq. (4-12) and obtaining the nonlinear frequency, the non-dimensionless variables are defined as follow:

$$\overline{A} \equiv \frac{A}{h},\ \overline{w} \equiv \frac{W_0}{h},$$

$$F_{Linear}^{\ 2} = \frac{E}{\rho R^2}\left[\frac{\xi^4}{(\xi^2+1)^2} + \frac{\varepsilon(\xi^2+1)^2}{12(1-\upsilon^2)}\right],$$

$$\xi = \frac{m\pi R}{nl}, \qquad (4\text{-}13)$$

$$\varepsilon = (\frac{n^2 h}{R})^2,$$

$$\Omega = \frac{\omega}{F_{Linear}}.$$

Where $\overline{A}$ is non-dimensionless amplitude, F_{Linear} is linear frequency, ξ is aspect ratio, ε is a nonlinear parameter, $\overline{w}$ is non-dimensionless initial imperfection, and *W* is the ratio of the nonlinear frequency to the linear frequency called non-dimensionless frequency either.

With substituting the aforementioned parameters in Eq. (4-13), non-dimensionless form of Eq. (4-12) is defined as:

$$-\Omega^2(b_1\overline{A}+b_2\overline{A}^3)+b_3\overline{A}+b_4\overline{A}^3+b_5\overline{A}^5=0 \tag{4-14}$$

b values are reported in Appendix B.4.

4.2. The Effects of Imperfection on the Nonlinear Dynamic of SWCNT based on the Nonlocal Theory

4.2.1. Modeling of SWCNT with an Initial Geometric Imperfection

Eringen's nonlocal elasticity is used to write the equations of motion in the nonlocal form and based on the complete explanation in chapter three and the below formula:

$$(1-(e_0a)^2\nabla^2)\sigma=t \tag{4-15}$$

$$\nabla^2=\frac{\partial^2}{\partial x^2}+\frac{1}{R^2}\frac{\partial^2}{\partial\theta^2}$$

Therefore, the nonlocal stress–strain relationships are in the following form:

$$\sigma_x-(e_0a)^2\nabla^2\sigma_x=\frac{E}{(1-\upsilon^2)}(\varepsilon_x+\upsilon\varepsilon_\theta)$$

$$\sigma_\theta-(e_0a)^2\nabla^2\sigma_\theta=\frac{E}{(1-\upsilon^2)}(\varepsilon_\theta+\upsilon\varepsilon_x) \tag{4-16}$$

$$\tau_{x\theta}-(e_0a)^2\nabla^2\tau_{x\theta}=\frac{E}{2(1+\upsilon)}\gamma_{x\theta}$$

The stress resultants in the nonlocal form are written as:

$$N_x = C(\varepsilon_x + \nu\varepsilon_\theta) + (e_0 a)^2 \nabla^2 N_x$$

$$N_\theta = C(\varepsilon_\theta + \nu\varepsilon_x) + (e_0 a)^2 \nabla^2 N_\theta \qquad (4\text{-}17)$$

$$N_{x\theta} = C\frac{(1-\upsilon)}{2}\gamma_{x\theta} + (e_0 a)^2 \nabla^2 N_{x\theta}$$

Based on Eq.(4-4), the above mentioned equations with considering an initial imperfection are written as:

$$N_x - (e_0 a)^2 \nabla^2 N_x = \frac{EH}{1-\upsilon^2}[-\frac{\upsilon w}{R} + \frac{1}{2}(\frac{\partial w}{\partial x})^2 + \frac{\partial w}{\partial x}\frac{\partial w_0}{\partial x} + \frac{\upsilon}{2}(\frac{\partial w}{R\partial\theta})^2 + \upsilon\frac{\partial w}{R\partial\theta}\frac{\partial w_0}{R\partial\theta} + \frac{\partial u}{\partial x} + \frac{\upsilon}{R}\frac{\partial \upsilon}{\partial\theta}]$$

$$N_\theta - (e_0 a)^2 \nabla^2 N_\theta = \frac{EH}{1-\upsilon^2}[-\frac{w}{R} + \frac{\nu}{2}(\frac{\partial w}{\partial x})^2 + \nu\frac{\partial w}{\partial x}\frac{\partial w_0}{\partial x} + \frac{1}{2}(\frac{\partial w}{R\partial\theta})^2 + \upsilon\frac{\partial u}{\partial x} + \frac{\partial w}{R\partial\theta}\frac{\partial w_0}{R\partial\theta} + \frac{1}{R}\frac{\partial \upsilon}{\partial\theta}] \qquad (4\text{-}18)$$

$$N_{x\theta} - (e_0 a)^2 \nabla^2 N_{x\theta} = \frac{EH}{2(1+\upsilon)}[\frac{1}{R}\frac{\partial u}{\partial\theta} + \frac{\partial w}{\partial x}\frac{\partial w_0}{R\partial\theta} + \frac{\partial w_0}{\partial x}\frac{\partial w}{R\partial\theta} + \frac{1}{R}\frac{\partial w}{\partial x}\frac{\partial w}{\partial\theta} + \frac{\partial \upsilon}{\partial x}]$$

The Donnell's equation of motion for the SWCNT with an initial geometric imperfection and based on nonlocal elasticity theory is derived based on the explanations in chapter three and the aforementioned new components:

$$D\nabla^4 w-\frac{1}{R}\frac{\partial^2 F}{\partial x^2}-(\frac{\partial^2 F}{R^2\partial\theta^2}(w_{,xx}+w_{0,xx})-\frac{2}{R^2}\frac{\partial^2 F}{\partial x\partial\theta}(w_{,x\vartheta}+w_{0,x\vartheta})+ \quad (4\text{-}19\text{-a})$$
$$\frac{1}{R^2}\frac{\partial^2 F}{\partial x^2}(w_{,\theta\theta}+w_{0,\theta\theta})=-\rho h\ddot{w}+\rho h(e_0 a)^2(\ddot{w}_{xx}+\frac{\ddot{w}_{\theta\theta}}{R^2})$$

$$\nabla^4 F-(e_0 a)^2(\nabla^6 F)= \quad (4\text{-}19\text{-b})$$
$$EH(-\frac{1}{R}\frac{\partial^2 w}{\partial x^2}+\frac{1}{R^2}\left[\left(\frac{\partial^2 w}{\partial x\partial\theta}\right)^2+2\frac{\partial^2 w}{\partial x\partial\theta}\frac{\partial^2 w_0}{\partial x\partial\theta}-(\frac{\partial^2 w}{\partial x^2}+\frac{\partial^2 w_0}{\partial x^2})\frac{\partial^2 w}{\partial\theta^2}-\frac{\partial^2 w}{\partial x^2}\frac{\partial^2 w_0}{\partial\theta^2}\right])$$

$$\nabla^4 w=(\frac{\partial^2 w}{\partial x^2}+\frac{1}{R^2}\frac{\partial^2 w}{\partial\theta^2})^2$$

$$\nabla^6 w=(\frac{\partial^2 w}{\partial x^2}+\frac{1}{R^2}\frac{\partial^2 w}{\partial\theta^2})^3$$

4.2.2. Solution Procedure

The solution procedure is the same as a solution which has been explained in section (4.1.2).For solving the nonlinear Donnell's equation with an initial imperfection and based on the nonlocal theory, the shape mode for radial displacement based on the simple boundary condition is defined as follow [66][17]:

$$w(x,\theta,t)=A(t)\cos(n\theta)\sin(\frac{m\pi x}{L})+\frac{n^2}{4R}A(t)^2\sin(\frac{m\pi x}{L})^2. \quad (4\text{-}20)$$

The initial imperfection has been considered as a simple model which represents the widespread defects on the carbon nanotube.

$$w_0(x,\theta) = W_0 \sin(n\theta)\sin(\frac{m\pi x}{L}) \tag{4-21}$$

By substituting Eq. (4-20) and Eq. (4-21) in the right-hand side of Eq. (4-19-b) and solving it the particular solution is:

$$F_p = EH(A_{11}\cos(2n\theta) + A_{22}\cos(n\theta)\sin(\frac{3m\pi x}{L}) + A_{33}\cos(n\theta)\sin(\frac{m\pi x}{L}) \tag{4-22}$$
$$+ A_{44}\sin(n\theta)\sin(\frac{3m\pi x}{L}) + A_{55}\sin(2n\theta) + A_{66}\sin(n\theta)\sin(\frac{m\pi x}{L})$$

Where A values are not reported here for the sake of brevity and can be found in Appendix B.5.

By substituting Eq. (4-20), Eq. (4-21) and Eq. (4-22) in Eq. (4-19-a), there is a complicated partial differential equation (PDE) which cannot be solved by the separation of variables. Therefore, it is necessary to use the numerical method for changing this partial differential equation (PDE) to ordinary differential equation (ODE).Then, the averaging method is used to solve the nonlinear ODE approximately.

For solving the averaged equation of motion and obtaining the nonlinear frequency, the non-dimensionless variables are defined as follow:

$$\bar{A} \equiv \frac{A}{h},\ \bar{w} \equiv \frac{W_0}{h},$$

$$F_{Linear}{}^2 = \frac{E}{\rho R^2 + \mu^2(\xi^2+1)}\left[\frac{\xi^4}{(\xi^2+1)^2 + \mu^2(\xi^2+1)^3} + \frac{\varepsilon(\xi^2+1)^2}{12(1-\upsilon^2)}\right],$$

$$\xi = \frac{m\pi R}{nl}, \tag{4-23}$$

$$\varepsilon = (\frac{n^2 h}{R})^2,$$

$$\overline{\mu} = \frac{(e_0 a)\times n}{R},$$

$$\Omega = \frac{\omega}{F_{Linear}}.$$

Where $\overline{A}$ is non-dimensionless amplitude, F_{Linear} is linear frequency based on nonlocal elasticity theory, ξ is aspect ratio, ε is a nonlinear parameter, $\overline{w}$ is a non-dimensionless initial imperfection, $\overline{\mu} = \frac{(e_0 a)\times n}{R}$ is a non-dimensionless nonlocal parameter, and Ω is the ratio of the nonlinear frequency to the linear frequency called non-dimensionless frequency either.

With substituting the aforementioned parameters in the averaged equation of motion, a non-dimensionless form of the equation is defined as:

$$-\Omega^2((1+\overline{\mu}^2 b_{11})\tilde{A} + b_{22}\tilde{A}^3) + b_{33}\tilde{A} + b_{44}\tilde{A}^3 + b_{55}\tilde{A}^5 = 0. \tag{4-24}$$

b values are reported in Appendix B.6.

4.3. Results Verification

The result of the present research has been verified by Liu [69]. In figure 4-1 the non-dimensional frequencies have been plotted against imperfection amplitude. Axial and circumferential wave numbers are *m=5* and *n=25*. The results have been verified by the figure. (4-2) which has been plotted by Liu [69].

4.4. Results and Discussion

For investigation dynamical behavior of SWCNT, three various zigzag SWCNT (10,0), (20,0) and (30,0) have been selected which the corresponding geometries have been reported by Gupta [53] which are shown in the table 3-2.

Maple software has been used for the derivation of equations of motion, Galerkin method and averaging method. Then, the related diagrams have been plotted using MATLAB software.

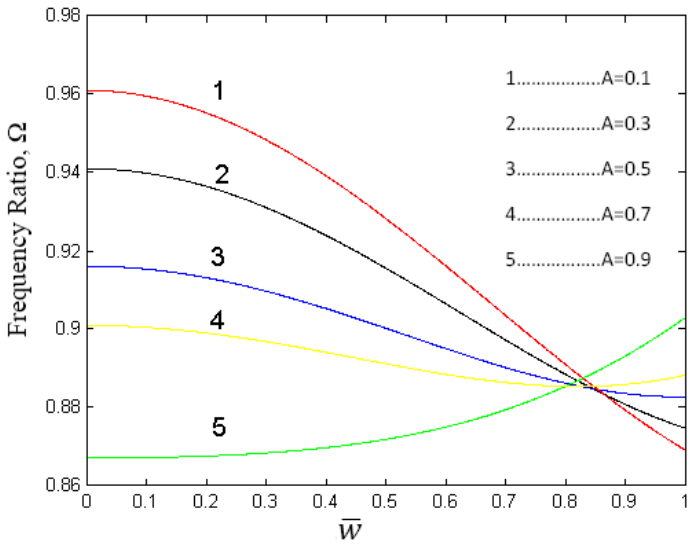

Figure 4-1: Non-dimensional Frequency against amplitude of imperfection for various amplitudes of vibration (Present work)

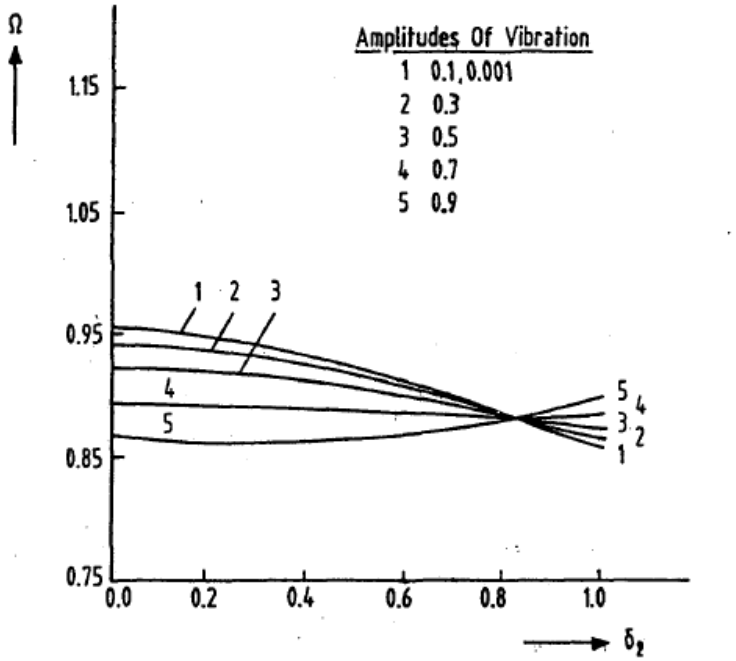

Figure 4-2: Non-dimensional Frequency against amplitude of imperfection for various amplitudes of vibration [69].

4.4.1. The Effect of Initial Geometric Imperfection on the Nonlinear Dynamic of (10,0) zigzag SWCNT based on Classical Theory

Figure 4-3 shows the effect of an initial geometric imperfection on the nonlinear frequency for (10,0) zigzag SWCNT. Aspect ratio is $\xi = 0.25$ and the axial and the circumferential wave numbers are *m=n=1*. Based on the results, the initial geometric imperfection increases nonlinearity in the system, and the nonlinear frequencies are increased by increasing an initial geometric imperfection. Figure 4-4 and figure 4-5 represent the effect of an initial imperfection for the lower and higher amplitudes respectively. It is seen that an initial imperfection increases the nonlinear frequency, and the difference between the nonlinear frequencies is more at the lower amplitudes and the area which the softening behavior changes to the hardening type, and it is reduced by increment the vibration amplitudes. However, it does not have any influence on the softening or hardening behavior of SWCNT.

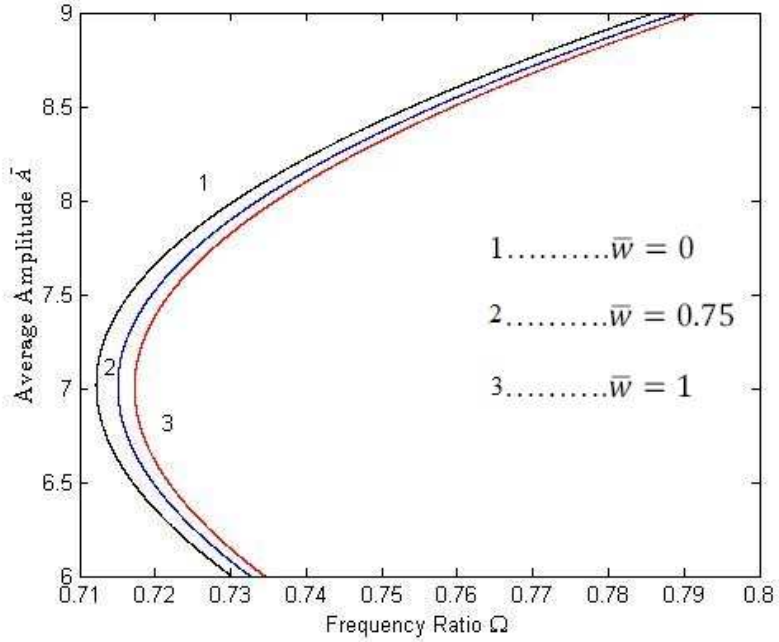

Figure 4-3: Effects of an initial geometric imperfection on the nonlinear vibration of (10,0) zigzag SWCNT.

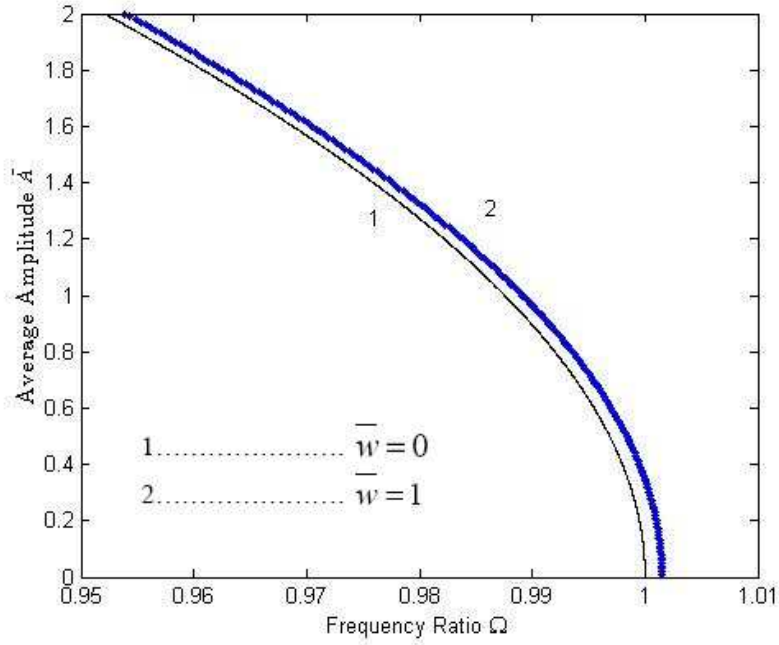

Figure 4-4: Effects of an initial geometric imperfection on the nonlinear vibration of (10,0) zigzag SWCNT at the lower amplitudes.

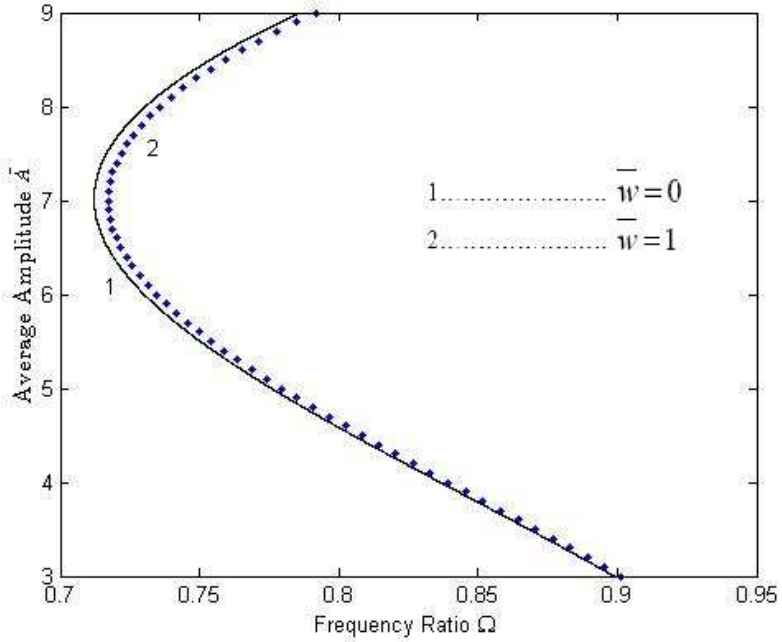

Figure 4-5: Effects of an initial geometric imperfection on the nonlinear vibration of (10,0) zigzag SWCNT at the higher amplitudes.

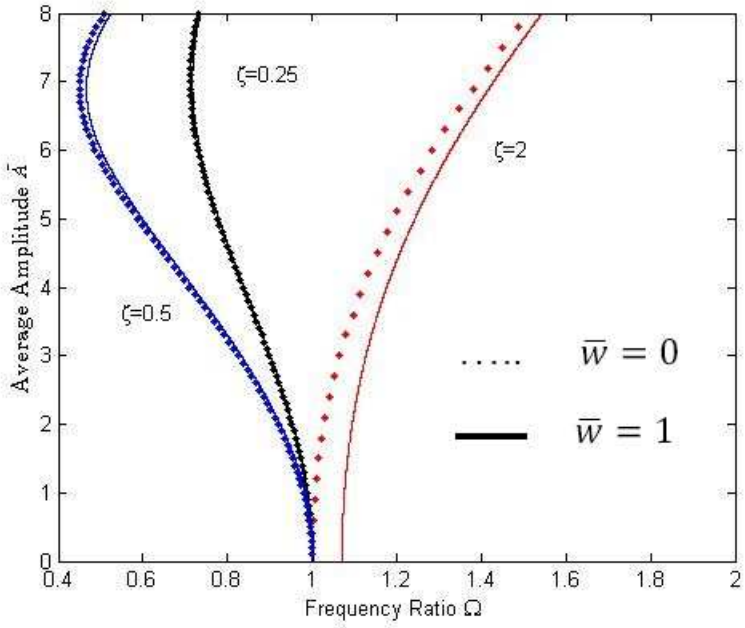

Figure 4-6: Effects of an initial geometric imperfection $\bar{w}=1$ on the nonlinear vibration of (10,0) zigzag SWCNT with the various aspect ratios $\xi = 0.25,0.5,2$.

4.4.2. The Effect of Initial Geometric Imperfection on the Nonlinear Dynamic of SWCNT with the Various Aspect Ratios based on Classical Theory

Figure 4-6 represents the effect of an initial geometric imperfection on the nonlinear behavior of (10,0) zigzag SWCNT with the various aspect ratios. Aspect ratios are $\xi = 0.25,0.5,2$ and the axial and the circumferential wave numbers are *m=n=1*. The results of the SWCNT with an initial geometric imperfection are compared with the perfect SWCNT to reach the findings of the research. An initial geometric imperfection is equal to $\overline{w} = 1$.It is seen that the influence of the imperfection is more for the shorter SWCNTs rather than longer ones. Also, it is observed that the difference between the frequency ratios decreased at the higher amplitudes. Moreover, an initial geometric imperfection does not have any impact on the type of vibration i.e. softening or hardening. It is softening type at the lower amplitude which changes to the hardening type at the higher amplitudes for long carbon nanotubes ($\xi = 0.25,0.5,2$). However, it is just hardening type for the short carbon nanotube ($\xi = 2$).

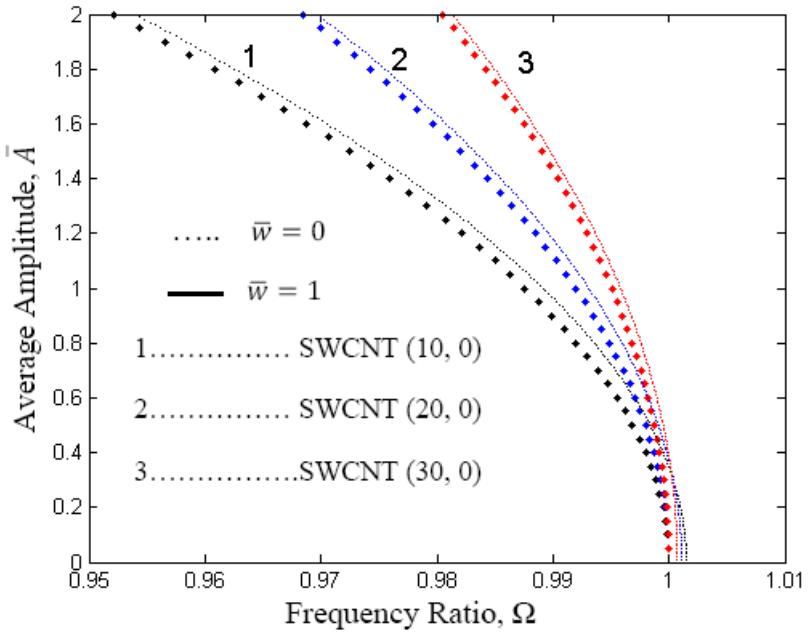

Figure 4-7: Effects of an initial geometric imperfection $\bar{w} = 1$ on nonlinear vibration of various SWCNT for aspect ratio $\xi = 0.25$.

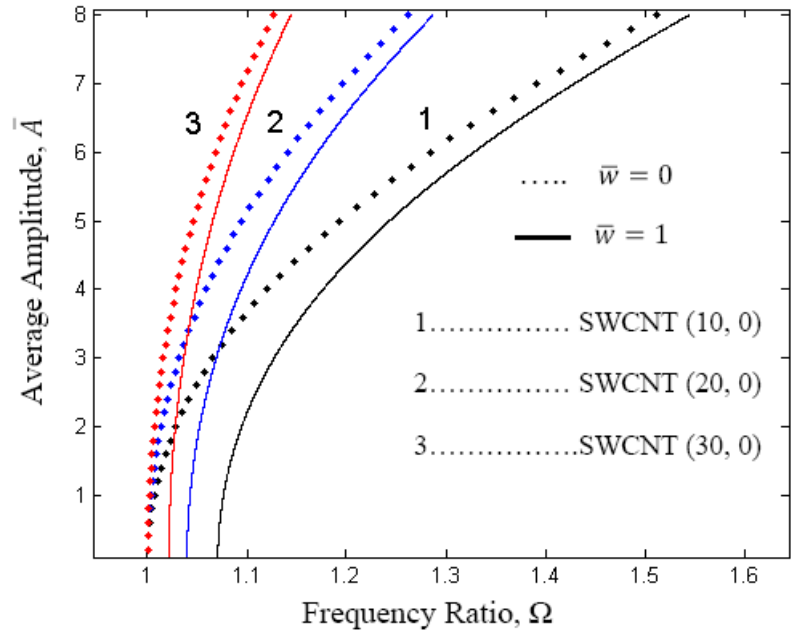

Figure 4-8: Effects of an initial geometric imperfection $\bar{w} = 1$ on the nonlinear vibration of various SWCNT for aspect ratio $\xi = 2$.

4.4.3. The Effect of Initial Geometric Imperfection on the Nonlinear Dynamic of SWCNT for the various SWCNTs based on Classical Theory

Effects of an initial geometric imperfection on the various SWCNTs have been shown in the figure 4-7 and figure. 4-8. For this purpose, three different (10,0) (20,0) and (30,0) zigzag SWCNT have been chosen and wave numbers are *m=1* and *n=1*. The aspect ratio is equal to $\xi = 0.25$ (long SWCNT) for the figure 4-7 and it is equal $\xi = 2$ (short SWCNT) for the figure 4-8. Both figures reveal that the effects of imperfection are more on the (10,0) zigzag SWCNT among the others. In fact (10,0) zigzag SWCNT has the bigger nonlinear parameter among the other SWCNTs

4.4.4. The Effect of an Initial Geometric Imperfection on the Nonlinear Dynamic Behavior of SWCNT for the various Wave Numbers based on Classical Theory

Figures 4-9 and figure 4-10 represent the effect of an initial geometric imperfection on the nonlinear behavior of SWCNT with various circumferential wave numbers. Circumferential wave numbers are $n = 1,2,5$ and the axial wave number is *m=1*. The length of SWCNT is $l = \pi R$ in figure 4-9 and it is equal to $l = 4\pi R$ in figure 4-10. It means that figure 4-9 represents the results for the shorter SWCNT. The result of the SWCNT with initial geometric imperfection equal to $\overline{w} = 1$ compared with the perfect SWCNT. It is found that the frequency difference between imperfect SWCNT and the perfect one is decreased by increment the wave numbers. Therefore, in the short nanotube

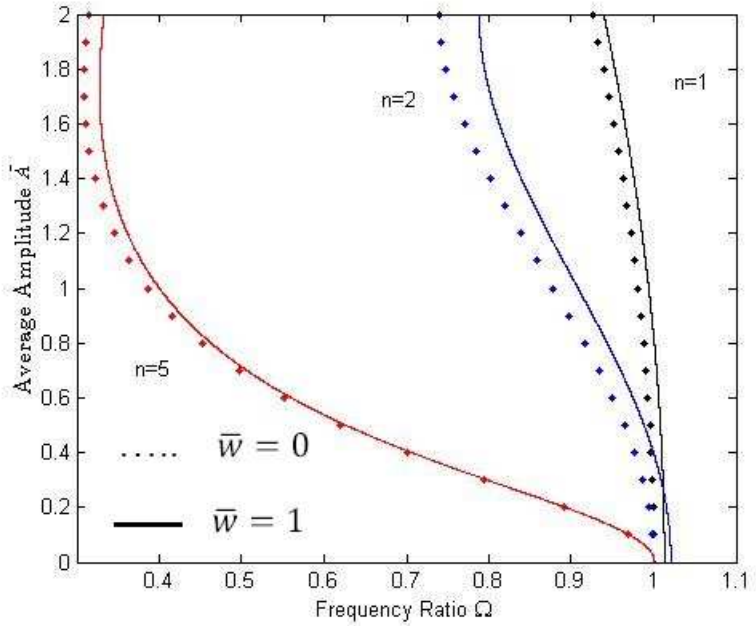

Figure 4-9: Effects of an initial geometric imperfection $\bar{w} = 1$ on the nonlinear vibration of various SWCNT for the various circumferential wave numbers $L = \pi R$.

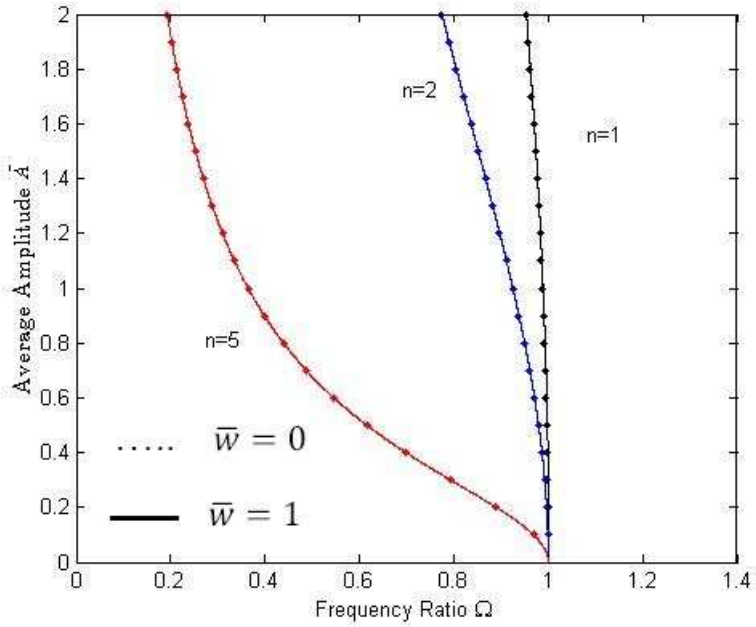

Figure 4-10**:** Effects of an initial geometric imperfection $\bar{w} = 1$ on the nonlinear vibration of various SWCNT for the various circumferential wave numbers $L = 4\pi R$.

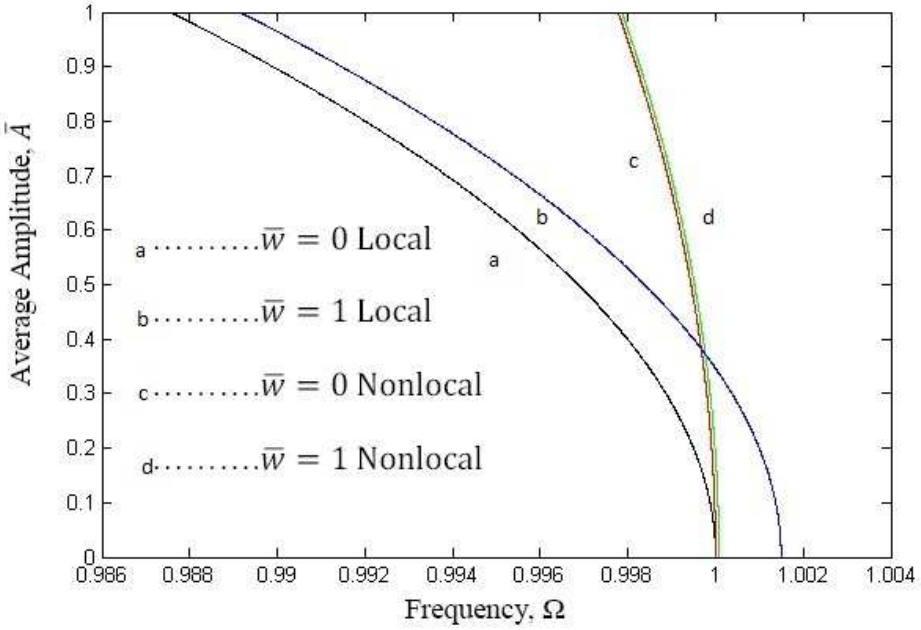

Figure 4-11: Effect of an initial geometric imperfection on the nonlinear behavior of zigzag (10,0) SWCNT based on both theories $\xi = 0.25$.

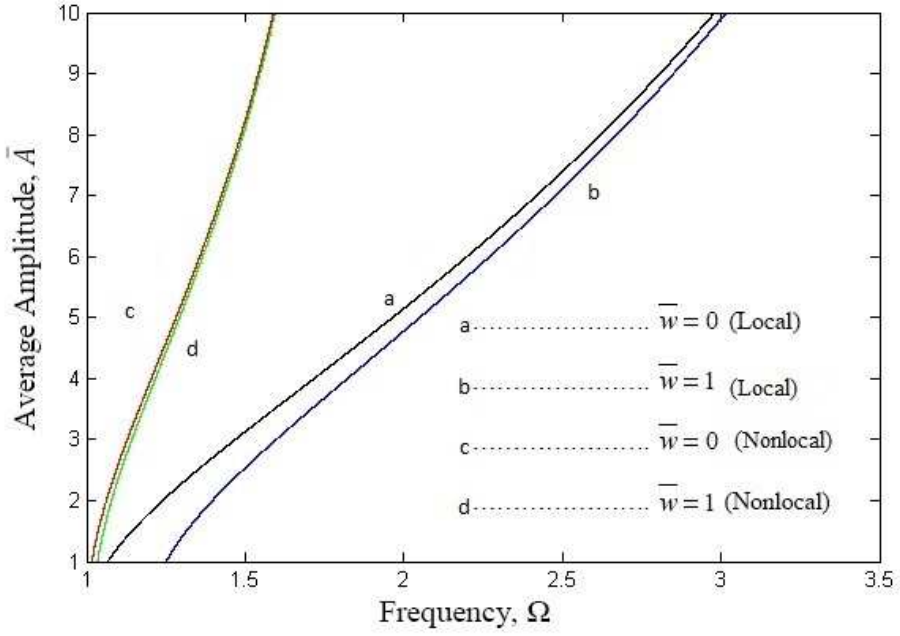

Figure 4-12: Effect of an initial geometric imperfection on the nonlinear behavior of zigzag (10,0) SWCNT based on both theories $\xi = 2$.

the effect of the initial geometric imperfection can be neglected for the bigger wave numbers.

4.4.5. The Comparison of the Effect of an Initial Geometric Imperfection on the Nonlinear Dynamic Behavior of SWCNT based on the Both Theories

Figures 4-11 and figure 4-12 compare the effects of an initial geometric imperfection on the nonlinear behavior of (10,0) zigzag SWCNT based on both local (classical) and nonlocal theories. Figure 4-11-a and figure 4-12-a represent the perfect SWCNT and figure 4-11-b and figure 4-12-b represent the SWCNT with an initial geometric imperfection based on the local theory. However, figure 4-11-c and figure 4-12-c show the perfect SWCNT, and figure 4-11-d and figure 4-12-d show the SWCNT with imperfection based on the nonlocal theory. The aspect ratio is equal to $\xi = 0.25$ (long SWCNT) for the figure 4-11 and it is equal $\xi = 2$ (short SWCNT) for the figure 4-12. Also, the wave numbers are equal to *m=n=1*. Based on both figures, the nonlinear behavior for the SWCNT with an initial geometric imperfection is approximately the same as the perfect one based on the nonlocal elasticity theory. The frequency ratio is increased at the lower amplitudes and decreased at the higher amplitudes for long SWCNT, and nonlocal parameter increases the frequencies at all amplitudes for the short SWCNT. Moreover, it was observed that the difference between the perfect SWCNT and the imperfect one is more based on the classical theory. It means that the errors for calculation the frequencies based on classical theory will arise if we do not consider an initial geometric imperfection.

5 Chapter 5: Conclusion and Recommendation for future works

5.1. Conclusion

The main purpose of this thesis was to investigate the nonlinear dynamic behavior of imperfect single-walled carbon nanotubes and to obtain the vibration frequencies with high accuracy and near to the experimental methods. Results indicated that an initial geometric imperfection plays an important role in the resulting carbon nanotubes frequencies. As a result, taking into account all of the mentioned parameters nonlinear effects, nonlocal elasticity theory and an initial geometric imperfection help to achieve the results with high accuracy.

In conclusion, the research can be concluded as follows:

- Nonlocal parameters decreased the nonlinearity in the system for both perfect and imperfect SWCNTs; however, the difference between the two theories reduced by increasing the length of SWCNT. Moreover, the dynamic behavior of SWCNT is softening type for the long CNTs at the lower amplitudes which have been changed to the hardening at the higher amplitudes. While the dynamic behavior of the short CNTs was hardening type.

- Nonlinearity was increased in the system by increasing the nonlinear parameters; however, it is less by using the nonlocal continuum mechanics. Also, the effect of imperfection increased by an increment of nonlinear parameters.

- An initial imperfection increased the nonlinearity in the system, and this increment was higher at the lower amplitudes and especially in the region which the nonlinear dynamic behavior changed from softening type to the hardening type. However, it does not affect the softening or hardening behavior of CNT.

- An initial geometric imperfection does not have any impact on the softening and hardening behavior.

- The difference between the frequency ratios decreased by using the bigger circumferential wave numbers. It means that the effect of initial geometric imperfection can be neglected at the bigger wave numbers.

- Incrementing of the circumferential wave numbers increases the nonlinear parameters and decreases the aspect ratios, but it has more effect on the nonlinear parameters. Therefore, it increased the nonlinearity in the system. Furthermore, the difference between the frequency ratios has been decreased by using the bigger circumferential wave numbers. It means that the effect of initial geometric imperfection can be neglected at the bigger wave numbers

- Although an initial geometric imperfection increased the nonlinearity in the system, the difference between the perfect and imperfect SWCNTs decreased by using the nonlocal theory. It means that we cannot neglect the effect of the initial geometric imperfection during the study of the dynamic behavior of CNTs with the classical theory.

To sum up, in order to design and manufacturing of the mechanical equipments with high accuracy, it is highly predominant to consider both the imperfection and the nonlocal elasticity theory at the same time. The error amid the theory and the experimental method will be reduced by using the two mentioned items in our calculations based on the previous figures.

5.2. Recommendation and Future Outlook

It is recommended that some researchers consider other shell theories such as Flugge and Sanders to study the nonlinear behavior of carbon nanotubes and compare the results with this thesis. It is also good if the future researchers consider the effect of others kinds of failure such as topological defect or holes in carbon nanotubes and using continuum shell theory. Furthermore, it is possible to expand this research for multi-walled carbon nanotubes. Another recommendation is considering the effect of the initial geometric imperfection on the nonlinear dynamic behavior of carbon nanotube coupled with fluid. It could be both fluid-filled carbon nanotube and carbon nanotubes conveying fluid.

List of References

[1] L. X. Zheng *et al.*, "Ultralong single-wall carbon nanotubes," *Nat. Mater.*, vol. 3, no. 10, pp. 673–676, 2004.

[2] S. Musso, "Growth and analysis on carbon nanomaterials," Politecnico de Torino, 2006.

[3] B. I. Yakobson and and P. Avouris, "Mechanical properties of carbon nanotubes," in *Carbon nanotubes*, vol. 272, no. 2001, Springer, 2001, pp. 287–327.

[4] A. Maiti, "Application of carbon nanotubes as electromechanical sensors-results from first-principles simulations," *Phys. Status Solidi B*, vol. 226, no. 1, pp. 87–93, 2001.

[5] D. S. Su and R. Schlögl, "Nanostructured carbon and carbon nanocomposites for electrochemical energy storage applications," *ChemSusChem*, vol. 3, no. 2, pp. 136–168, 2010.

[6] Sumio Iijima, "Helical microtubles of graphitic carbon," *Lett. To Nat.*, 1991.

[7] S. Kang and A. S. Brady-este, *Carbon nanotubes Basic Concepts and Physical Properties*. 2008.

[8] P. Poncharal, Z. L. Wang, D. Ugarte, and W. A. de Heer, "Electrostatic deflections and electromechanical resonances of carbon nanotubes," *Science (80-.).*, vol. 283, no. 5407, pp. 1513–1516, 1999.

[9] R. V. Seidel *et al.*, "Sub 20 nm Short Channel Carbon Nanotube Transistors," *Nano Lett.*, vol. 5, pp. 147–150, 2005.

[10] D. Qian, E. C. Dickey, R. Andrews, and T. Rantell, "Load transfer and deformation mechanisms in carbon nanotube-polystyrene composites," *Appl. Phys.*

Lett., vol. 76, no. 20, p. 2868, 2000.

[11] S. Supple and N. Quirke, “Rapid Imbibition of Fluids in Carbon Nanotubes,” *Phys. Rev. Lett.*, vol. 90, no. 21, p. 214501, 2003.

[12] T. A. Hilder and J. M. Hill, “Carbon nanotubes as drug delivery nanocapsules,” *Curr. Appl. Phys.*, vol. 8, no. 3–4, pp. 258–261, 2008.

[13] T. A. Hilder and J. M. Hill, “Modeling the loading and unloading of drugs into nanotubes,” *Small*, vol. 5, no. 3, pp. 300–308, 2009.

[14] P. G. Collins, “Defects and Disorder in Carbon Nanotubes,” *Oxford Handb. Nanosci. Technol. Front. Adv.*, pp. 1–73, 2009.

[15] T. Ebbesen and T. Takada, “Topological and sp 3 defect structures in nanotubes,” *Carbon N. Y.*, vol. 33, no. 7, pp. 973–978, 1995.

[16] Y. Kinoshita, M. Kawachi, T. Matsuura, and N. Ohno, “Axial buckling behavior of wavy carbon nanotubes : A molecular mechanics study,” *Phys. E Low-dimensional Syst. Nanostructures*, vol. 54, pp. 308–312, 2013.

[17] W. A. Nash, “Influence of initial geometric imperfections on vibrations of thin circular cylindrical shells,” *Comput. Struct.*, vol. 16, no. 1, pp. 125–130, 1983.

[18] K. Tunvir, A. Kim, and S. H. Nahm, “The effect of two neighboring defects on the mechanical properties of carbon nanotubes,” 2008.

[19] B. Arash and R. Ansari, “Evaluation of nonlocal parameter in the vibrations of single-walled carbon nanotubes with initial strain,” *Phys. E Low-Dimensional Syst. Nanostructures*, vol. 42, no. 8, pp. 2058–2064, 2010.

[20] R. Gao, Z. L. Wang, Z. Bai, W. A. De Heer, L. Dai, and M. Gao, “Nanomechanics of Individual Carbon Nanotubes from Pyrolytically Grown Arrays,” pp. 1–4, 2000.

[21] S. T. Purcell, P. Vincent, C. Journet, and V. T. Binh, “Tuning of Nanotube Mechanical Resonances by Electric Field Pulling,” pp. 1–4, 2002.

[22] B. I. Yakobson, M. P. Campbell, C. J. Brabec, and J. Bernholc, “High strain rate fracture and C-chain unraveling in carbon nanotubes,” *Comput. Mater. Sci.*, vol. 8, pp. 341–348, 1997.

[23] L. G. Zhou and S. Q. Shi, “Molecular dynamic simulations on tensile mechanical properties of single-walled carbon nanotubes with and without hydrogen storage,” vol. 23, pp. 166–174, 2002.

[24] D. Qian, G. J. Wagner, W. K. Liu, M.-F. Yu, and R. S. Ruoff, “Mechanics of carbon nanotubes,” *Appl. Mech. Rev.*, vol. 55, no. 6, p. 495, 2002.

[25] J. Peng, J. Wu, K. C. Hwang, J. Song, and Y. Huang, “Can a single-wall carbon nanotube be modeled as a thin shell?,” *J. Mech. Phys. Solids*, vol. 56, no. 6, pp. 2213–2224, 2008.

[26] Y. Zhang, G. Liu, and X. Han, “Transverse vibrations of double-walled carbon nanotubes under compressive axial load,” vol. 340, pp. 258–266, 2005.

[27] M. A. Gdu and M. C. Ece, “Vibration and Buckling of In-Plane Loaded Double-Walled Carbon,” vol. 31, pp. 305–310, 2007.

[28] C. Sun and K. Liu, “Vibration of multi-walled carbon nanotubes with initial axial loading,” vol. 143, pp. 202–207, 2007.

[29] Y. Yan, W. Q. Wang, and L. X. Zhang, “Noncoaxial vibration of fluid-filled multi-walled carbon nanotubes,” *Appl. Math. Model.*, vol. 34, no. 1, pp. 122–128, 2010.

[30] R. Ansari and M. Hemmatnezhad, “Nonlinear vibrations of embedded multi-walled carbon nanotubes using a variational approach,” *Math. Comput. Model.*,

vol. 53, no. 5–6, pp. 927–938, 2011.

[31] P. Soltani, J. Saberian, R. Bahramian, and A. Farshidianfar, “Nonlinear free and forced vibration analysis of a single-walled carbon nanotube using shell model,” vol. 1, no. 3, pp. 47–52, 2011.

[32] P. Zhang, Y. Huang, H. Gao, and K. C. Hwang, “Fracture Nucleation in Single-Wall Carbon Nanotubes Under Tension: A Continuum Analysis Incorporating Interatomic Potentials,” *J. Appl. Mech.*, vol. 69, no. 4, p. 454, 2002.

[33] P. Zhang, Y. Huang, P. H. Geubelle, P. A. Klein, and K. C. Hwang, “The elastic modulus of single-wall carbon nanotubes: A continuum analysis incorporating interatomic potentials,” *Int. J. Solids Struct.*, vol. 39, no. 13–14, pp. 3893–3906, 2002.

[34] A. Cemal Eringen, “Linear Theory of Nonlocal Elasticity and Dispersion of Plane Wave,” *Int. J. Eng. Sci.*, vol. 10, pp. 425–435, 1972.

[35] A. Cemal Eringen, “On differential equations of nonlocal elasticity and solutions of screw dislocation and surface wave,” *J. Appl. Mech.*, vol. 54, pp. 4703–4710, 1983.

[36] J. Peddieson, G. R. Buchanan, and R. P. McNitt, “Application of nonlocal continuum models to nanotechnology,” *Int. J. Eng. Sci.*, vol. 41, no. 3–5, pp. 305–312, 2003.

[37] A. Cemal Eringen, *Nonlocal Continuum Field Theories*. New York: Springer, 2002.

[38] L. J. Sudak, “Column buckling of multiwalled carbon nanotubes using nonlocal continuum mechanics,” *J. Appl. Phys.*, vol. 94, no. 11, pp. 7281–7287, 2003.

[39] A. M. Zenkour, “Nonlocal thermoelasticity theory without energy dissipation for nano-machined beam resonators subjected to various boundary conditions,” *Microsyst. Technol.*, vol. 23, no. 1, pp. 55–65, 2017.

[40] L. L. Ke, Y. Xiang, J. Yang, and S. Kitipornchai, “Nonlinear free vibration of embedded double-walled carbon nanotubes based on nonlocal Timoshenko beam theory,” *Comput. Mater. Sci.*, vol. 47, no. 2, pp. 409–417, 2009.

[41] B. Fang, Y. Zhen, C. Zhang, and Y. Tang, “Nonlinear vibration analysis of double-walled carbon nanotubes based on nonlocal elasticity theory,” *Appl. Math. Model.*, vol. 37, no. 3, pp. 1096–1107, 2013.

[42] A. G. Arani, M. S. Zarei, S. Amir, and Z. K. Maraghi, “Nonlinear nonlocal vibration of embedded DWCNT conveying fluid using shell model,” *Phys. B Phys. Condens. Matter*, vol. 410, pp. 188–196, 2013.

[43] P. Soltani, J. Saberian, and R. Bahramian, “Nonlinear Vibration Analysis of Single-Walled Carbon Nanotube With Shell Model Based on the Nonlocal Elasticity Theory,” vol. 11, no. January, pp. 1–10, 2016.

[44] Y. Wang, Y. Wang, and L. Ke, “Nonlinear vibration of carbon nanotube embedded in viscous elastic matrix under parametric excitation by nonlocal continuum theory,” vol. 83, pp. 195–200, 2016.

[45] Y. Hirai *et al.*, “Molecular dynamics studies on mechanical properties of carbon nano tubes with pinhole defects,” *Japanese J. Appl. Phys. Part 1-Regular Pap. Short Notes Rev. Pap.*, vol. 42, no. 6B, pp. 4120–4123, 2003.

[46] T. Dumitrica and B. I. Yakobson, “Strain-rate and temperature dependent plastic yield in carbon nanotubes from ab initio calculations,” *Appl. Phys. Lett.*, vol. 84,

no. 15, pp. 2775–2777, 2004.

[47] S. L. Mielke *et al.*, "The role of vacancy defects and holes in the fracture of carbon nanotubes," *Chem. Phys. Lett.*, vol. 390, no. 4–6, pp. 413–420, 2004.

[48] S. Zhang *et al.*, "Mechanics of defects in carbon nanotubes: Atomistic and multiscale simulations," *Phys. Rev. B - Condens. Matter Mater. Phys.*, vol. 71, no. 11, pp. 1–12, 2005.

[49] K. I. Tserpes and P. Papanikos, "TENSILE BEHAVIOR AND FRACTURE OF CARBON NANOTUBES CONTAINING STONE-WALES DEFECTS," in *Fracture of Nano and Engineering Materials*, 2006, pp. 39–40.

[50] H. S. Shen and C. L. Zhang, "Postbuckling of double-walled carbon nanotubes with temperature dependent properties and initial defects under combined axial and radial mechanical loads," *Int. J. Solids Struct.*, vol. 44, no. 5, pp. 1461–1487, 2007.

[51] H. S. Shen and C. L. Zhang, "Torsional buckling and postbuckling of double-walled carbon nanotubes by nonlocal shear deformable shell model," *Compos. Struct.*, vol. 92, no. 5, pp. 1073–1084, 2010.

[52] A. Farshidianfar and P. Soltani, "Nonlinear flow-induced vibration of a SWCNT with a geometrical imperfection," *Comput. Mater. Sci.*, vol. 53, no. 1, pp. 105–116, 2012.

[53] B. Wang, Z. C. Deng, and K. Zhang, "Nonlinear vibration of embedded single-walled carbon nanotube with geometrical imperfection under harmonic load based on nonlocal Timoshenko beam theory," *Appl. Math. Mech. (English Ed.*, vol. 34, no. 3, pp. 269–280, 2013.

[54] H. Mohammadi, M. Mahzoon, M. Mohammadi, and M. Mohammadi, "Postbuckling instability of nonlinear nanobeam with geometric imperfection embedded in elastic foundation," *Nonlinear Dyn.*, vol. 76, no. 4, pp. 2005–2016, 2014.

[55] M. Rafiee, X. Q. He, and K. M. Liew, "Non-linear dynamic stability of piezoelectric functionally graded carbon nanotube-reinforced composite plates with initial geometric imperfection," *Int. J. Non. Linear. Mech.*, vol. 59, pp. 37–51, 2014.

[56] H. L. Wu, J. Yang, and S. Kitipornchai, "Nonlinear vibration of functionally graded carbon nanotube-reinforced composite beams with geometric imperfections," *Compos. Part B Eng.*, vol. 90, pp. 86–96, 2016.

[57] I. Eshraghi, S. Jalali, and N. Pugno, "Imperfection Sensitivity of Nonlinear Vibration of Curved Single-Walled Carbon Nanotubes Based on Nonlocal Timoshenko Beam Theory," *Materials (Basel).*, vol. 9, no. 9, p. 786, 2016.

[58] A. Y. Joshi, A. Bhatnagar, S. C. Sharma, and S. P. Harsha, "Vibratory Analysis of a Doubly Clamped Wavy Single Walled Carbon Nanotube based Nano Mechanical Sensors," *Int. J. Eng. Sci.*, vol. 2, no. 5, pp. 993–1000, 2010.

[59] M. Amabili, *Nonlinear Vibrations and Stability of Shells and Plates*. Cambridge University Press, 2008.

[60] W.Leissa, *Vibration of Shells*. Washington DC: National Aeronautics And Space Administration, 1973.

[61] J. N. Reddy, *Energy Principles and Variational Methods in Applied Mechanics, 2nd Edition*. 2002.

[62] A. Love, “The Mathematical Theory of Elasticity,” vol. I, 1892.

[63] M. Amabili, “A comparison of shell theories for large-amplitude vibrations of circular cylindrical shells: Lagrangian approach,” *J. Sound Vib.*, vol. 264, no. 5, pp. 1091–1125, 2003.

[64] K. N. Karagiozis, M. P. Païdoussis, and M. Amabili, “Effect of geometry on the stability of cylindrical clamped shells subjected to internal fluid flow,” *Comput. Struct.*, vol. 85, no. 11–14, pp. 645–659, 2007.

[65] J. Soltani, P, Bahramian, R, Saberian, “Nonlinear Vibration Analysis of the Fluid-Filled Single Walled Carbon Nanotube with the Shell Model Based on the Nonlocal Elacticity Theory,” *J. Solid Mech.*, vol. 7, no. 1, pp. 58–70, 2015.

[66] D. Evensen, “NONLINEAR FLEXURAL VIBRATIONS OF THIN-WALLED CIRCULAR CYLINDERS,” *Natl. Aeronaut. Sp. Admijistrationsp. ADMIJISTRATION*, no. August 1967.

[67] A. H. Nayfeh and D. T. Mook, *Nonlinear Oscillations*. 1985.

[68] S. S. Gupta, F. G. Bosco, and R. C. Batra, “Wall thickness and elastic moduli of single-walled carbon nanotubes from frequencies of axial, torsional and inextensional modes of vibration,” *Comput. Mater. Sci.*, vol. 47, no. 4, pp. 1049–1059, 2010.

[69] D. . Liu, “Nonlinear vibrations of imperfect thin-walled cylindrical shells,” Delft University of Technology, 1988.

Appendix A

Appendix A.1

$$I = \rho h$$

$$A_1 = \frac{.l^6.R^6}{2.R^3.l^2.(16.n^4.l^6.R^2 + 64.(ea)^2.n^6.l^6)}.(m^2.R.n^2.\pi\ .(-A(t)^2))$$

$$A_2 = \frac{R^6.l^6}{\left[\begin{array}{l} 81.m^4.\pi^4.R^6.l^2 + n^4.l^6.R^2 + 18.m^2.\pi^2.n^2.l^4 \\ .R^4 + 729.(ea)^2.m^6.\pi^6.R^6 + 243.(ea)^2.n^2.m^4.\pi^4.l^2.R^4 + 27 \\ .(ea)^2.n^4.m^2.\pi^2.l^4.R^2 + (ea)^2.n^6.l^6 \end{array}\right]}.\left(\frac{m^2.\pi^2.n^4.A(t)^3}{4.R^3.l^2}\right)$$

$$A_3 = \frac{R^6.l^6}{\left[\begin{array}{l} R^3.l^2.(m^4.\pi^4.l^2.R^6 + n^4.l^6.R^2 + 2.m^2.\pi^2.n^2 \\ .l^4.R^4 + (ea)^2.n^6.l^6 + (ea)^2.m^6.\pi^6.R^6 + 3.(ea)^2.n^2.m^4.\pi^4 \\ .l^2.R^4 + 3.(ea)^2.n^4.m^2.\pi^2.l^4.R^2) \end{array}\right]}.\left(\frac{m^2.\pi^2.A(t)}{2}.\left(2.R^2 - \frac{n^4.A(t)^2}{2}\right)\right)$$

Appendix A.2

$$\gamma_1 = \frac{1}{2}\frac{\pi D(m^4\pi^4R^4 + l^4n^4 + 2n^2m^2\pi^2l^2R^2)}{R^3l^3}$$

$$\gamma_2 = \frac{1}{2}\frac{\pi^5 Dn^4m^4}{Rl^3}$$

$$\gamma_3 = \frac{3}{16}\frac{\pi I \ln^4}{R}$$

$$\gamma_4 = \frac{1}{2}\pi IlR$$

$$\gamma_5 = \frac{3}{16}\frac{\pi I \ln^4}{R}$$

$$\gamma_6 = \frac{1}{4}\frac{\pi^3 In^4m^2}{Rl}$$

$$\gamma_7 = \frac{1}{4}\frac{\pi^3 In^4 m^2}{Rl}$$

$$\gamma_8 = \frac{1}{2}\frac{\pi I(l^2 n^2 + R^2 m^2 \pi\ )}{Rl}$$

$$\gamma_9 = -\frac{3}{16} R\pi^5 m^4 (41R^6 m^4 \pi^4 l^2 + 10R^4 m^2 \pi^2 l^4 n^2 + R^2 l^6 n^4) n^8 l^3$$

$$\gamma_{10} = -\frac{3}{16} R\pi^5 m^4 (365m^6 \pi^6 R^6 + 123m^4 \pi^4 R^4 n^2 l^2 + 15l^4 n^4 m^2 \pi^2 R^2 + n^6 l^6) n^8 l^3$$

$$\gamma_{11} = -\frac{1}{32} R^3 (81R^{12} m^{\ 8} \pi^8 l^4 - 15R^4 l^{12} n^8 - 1178R^8 m^4 \pi^4 l^8 n^4 - 268R^6 m^2 \pi^2 l^{10} n^6 + 180R^{10} m^6 \pi^6 l^6 n^2) m^4 \pi^5$$

$$\gamma_{12} = -\frac{1}{16} R^5 l^2 (405R^{10} m^{10} \pi^{10} - 39n^{10} l^{10} - 767n^8 l^8 R^2 m^2 \pi - 5062R^6 m^6 \pi^6 l^4 n^4) m^4 \pi^5$$

$$\gamma_{13} = -\frac{1}{32} R^3 (729R^{12} m^{12} \pi^{12} - 63l^{12} n^{12} - 15225R^4 m^4 \pi^4 l^8 n + 2430R^{10} m^{10} \pi^{10} n^2 l^2 - 45116R^6 m^6 \pi^6 l^6 n^6$$
$$- 1698R^2 m^2 \pi^2 l^{10} n^{10} + 2943R^8 m^8 \pi^8 n^4 l^4)$$

$$\gamma_{14} = -\frac{1}{32} (288R^{10} m^2 \pi^2 l^{10} n^2 + 1296R^{12} m^4 \pi^4 l^8 + 16R^8 l^{12} n^4) m^4 \pi^5 R$$

$$\gamma_{15} = -\frac{1}{2} R^7 l^6 (99R^2 m^2 \pi^2 l^4 n^4 + 567R^4 m^4 \pi^4 l^2 n^2 + 729R^6 m^6 \pi^6 + 5l^6 n^6) m^4 \pi^5$$

$$\gamma_{16} = -2R^5 l^6 n^2 (27R^2 m^2 \pi^2 l^4 n^4 + 729R^6 m^6 \pi^6 + 243R^4 m^4 \pi^4 l^2 n^2 + l^6 n^6) m^4 \pi^5$$

$$\gamma_{17} = (R^2 + 4(e_0 a)^2 n^2).l^3 (R^4 l^4 (R^2 \pi^2 m^2 + l^2 n^2)^2 (9R^2 \pi^2 m^2 + l^2 n^2)^2)$$

$$\gamma_{18} = 2(R^2 + 4(e_0 a)^2 n^2).l^3 (R^2 l^2 (5R^2 \pi^2 m^2 + l^2 n^2)^2 (9R^2 \pi^2 m^2 + l^2 n^2)^2 (R^2 \pi^2 m^2 + l^2 n^2)^2)$$

$$\gamma_{19} = (R^2 + 4(e_0 a)^2 n^2).l^3 ((R^2 \pi^2 m^2 + l^2 n^2)^3 (9R^2 \pi^2 m^2 + l^2 n^2) 3)$$

Appendix A.3

$$\overline{\alpha}_1 = \frac{1}{2}\frac{\pi^2 D(m^4 \pi^4 R^4 + l^4 n^4 + 2n^2 m^2 \pi^2 l^2 R^2)}{R^3 l^3}$$

$$\overline{\alpha}_2 = \frac{3}{8}\frac{\pi^6 D n^4 m^4}{R l^3}$$

$$\overline{\alpha}_3 = \frac{-9}{64}\frac{\pi^2 I \ln^4}{R}$$

$$\overline{\alpha}_4 = \frac{-1}{2}\pi^2 I l R$$

$$\overline{\alpha}_5 = \frac{-1}{8}\frac{\pi^4 I n^4 m^2}{R l}$$

$$\overline{\alpha}_6 = \frac{-1}{2}\frac{\pi^2 I (l^2 n^2 + R^2 m^2 \pi\ )}{R l}$$

$$\overline{\alpha}_7 = \frac{-3}{128}\pi^6 R^7 m^4 l^4 h E((R^2\pi^2 m^2 + 5 l^2 n^2)^2 (R^2\pi^2 m^2 - 3 l^2 n^2)(9R^2\pi^2 m^2 + l^2 n^2)^2)$$

$$\overline{\alpha}_8 = \frac{-1}{2}\pi^6 R^9 m^4 l^8 h E(l^2 n^2 + 9R^2 m^2 \pi^2)^2$$

$$\overline{\alpha}_9 = \frac{-15}{128}\pi^6 R^5 m^4 l^8 n^8 h E(41R^4\pi^4 m^4 + l^4 n^4 + 10R^2\pi^4 m^2 l^2 n^2)$$

$$\overline{\alpha}_{10} = \frac{-1}{2}\pi^6 R^7 m^4 l^6 h E((9R^2\pi^2 m^2 + 5 l^2 n^2)(9R^2\pi^2 m^2 + l^2 n^2)^2)$$

$$\overline{\alpha}_{11} = -2\pi^6 R^5 m^4 l^6 n^2 h E((9R^2\pi^2 m^2 + l^2 n^2)^3)$$

$$\overline{\alpha}_{12} = \frac{-3}{64}\pi^6 R^5 m^4 l^2 h E((5R^4\pi^4 m^4 + 26 l^2 n^2 R^2\pi^2 m^2 + 13 l^4 n^4)\ (R^2\pi^2 m^2 - 3 l^2 n^2)(9R^2\pi^2 m^2 + l^2 n^2)^2)$$

$$\overline{\alpha}_{13} = -\frac{15}{128} R^3\pi^6 m^4 l^6 n^8 h E(365R^6 m^6\pi^6 + 287R^4 m^2\pi^4 l^2 n^2 + 55R^2 m^2\pi^2 n^4 l^4 + 51 l^6 n^6)$$

$$\overline{\alpha}_{14} = \frac{-3}{128}\pi^6 R^3 m^4 h E((R^4\pi^4 m^4 + 6 l^2 n^2 R^2\pi^2 m^2 + 21 l^4 n^4)\ (R^2\pi^2 m^2 - 3 l^2 n^2)(9R^2\pi^2 m^2 + l^2 n^2)^2)$$

$$\overline{\alpha}_{15} = \frac{-15}{32}\pi^6 R m^4 n^{10} l^6 h E((73R^4\pi^4 m^4 + l^4 n^4 + 10 l^2 n^2 R^2 m^2\pi^2)(5R^2\pi^2 m^2 + l^2 n^2))$$

$$\overline{\alpha}_{16} = R^6 l^7((9R^2\pi^2m^2 + l^2n^2)^2(9R^2\pi^2m^2 + l^2n^2)^2)$$

$$\overline{\alpha}_{17} = -2R^4 l^5((5R^2\pi^2m^2 + 3l^2n^2)\ (R^2\pi^2m^2 + l^2n^2)^2(9R^2\pi^2m^2 + l^2n^2)^2)$$

$$\overline{\alpha}_{18} = R^2 l^3(50R^2l^2\pi^2m^2n^2 + 9l^4n^4 + 9R^4m^4\pi^4)\ (9R^2\pi^2m^2 + l^2n^2)^2(R^2\pi^2m^2 + l^2n^2)^2)$$

$$\overline{\alpha}_{19} = 4n^2 l^3((R^2\pi^2m^2 + l^2n^2)^3(9R^2\pi^2m^2 + l^2n^2)^3)$$

Appendix A.4

$$b_1 = (\xi^2 + 1)$$

$$b_2 = \frac{3.\varepsilon}{16} + \frac{\varepsilon.\mu^2.(\xi^2)}{4}$$

$$b_3 = 2\left(\frac{\varepsilon.(\xi^2+1)^2}{12(1-\nu^2)} + \frac{\xi^4}{(\xi^2+1)^2 + \mu^2.(\xi^2+1)^3}\right)$$

$$b_4 = \frac{3.\varepsilon^2.\xi^4}{24(1-\nu^2)} + \frac{3}{32}\frac{\varepsilon\xi^4(\mu^2\xi^6 + 3\mu^2\xi^4 + \xi^4 + 2\xi^2 + 3\mu^2\xi^2 - 63\mu^2 - 15)\varepsilon\xi^4)}{(4\mu^4\xi^6 + \mu^2\xi^6 + 12\mu^4\xi^4 + 7\mu^2\xi^4 + \xi^4 + 12\mu^4\xi^2 + 11\mu^2\xi^2 + 2\xi^2 + 4\mu^4 + 5\mu^2 + 1)}$$

$$b5 = \frac{15}{32}\frac{(\xi^4\varepsilon^2(\mu^2 + 365\mu^2\xi^6 + 15\mu^2\xi^2 + 1 + 123\mu^2\xi^4 + 10\xi^2 + 41\xi^4))}{\left[\begin{array}{l}(810\mu^2\xi^{10} + 1962\mu^2\xi^8 + 1540\mu^2\xi^6 + 436\mu^2\xi^4 + 50\mu^2\xi^2 + 1540\mu^4\xi^6 + 327\mu^4\xi^4 + 30\mu^4\xi^2 \\ 2430\mu^4\xi^{10} + 2943\mu^4\xi^8 + 1 + 2\mu^2 + 729\mu^4\xi^{12} + 81\xi^8 + 118\xi^4 + 180\xi^6 + 20\xi^2 + \mu^4)\end{array}\right]}$$

Appendix B

Appendix B.1

$$A1 = \frac{1}{4}\frac{l^2 m^2 n^4 \pi^2 A(t)^2 W_0}{\left(81m^4\pi^4 + \frac{n^4 l^4}{R^4} + \frac{18m^2\pi^2 n^2 l^2}{R^2}\right)R^3}$$

$$A2 = \frac{1}{4}\frac{l^2 m^2 \pi^2 n^4 A(t)^3}{\left(81m^4\pi^4 + \frac{n^4 l^4}{R^4} + \frac{18m^2\pi^2 n^2 l^2}{R^2}\right)R^3}$$

$$A3 = -\frac{1}{4}\frac{l^2 m^2 n^4 \pi^2 A(t)^2 W_0}{\left(m^4\pi^4 + \frac{n^4 l^4}{R^4} + \frac{2m^2\pi^2 n^2 l^2}{R^2}\right)R^3}$$

$$A4 = \frac{l^2\left(m^2\pi^2 RA(t) - \frac{1}{4}\frac{m^2\pi^2 n^4 A(t)^3}{R}\right)}{\left(m^4\pi^4 + \frac{n^4 l^4}{R^4} + \frac{2m^2\pi^2 n^2 l^2}{R^2}\right)R^2}$$

$$A5 = -\frac{1}{32}\frac{R^2 m^2 \pi^2 A(t)^2}{n^2 l^2}$$

$$A6 = -\frac{1}{16}\frac{R^2 m^2 \pi^2 W_0 A(t)}{n^2 l^2}$$

Appendix B.2

$$I = \rho h$$

$$\tilde{\alpha}_1 = \frac{1}{2}\frac{\pi^5 D}{Rl^3}$$

$$\tilde{\alpha}_2 = \frac{1}{2}\frac{\pi D(\pi^4 R^4 + l^4 + 2\pi^2 l^2 R^2)}{l^3 R^3}$$

$$\tilde{\alpha}_3 = \frac{3}{16}\frac{\pi I l}{R}$$

$$\tilde{\alpha}_4 = \frac{3}{16}\frac{\pi I l}{R}$$

$$\tilde{\alpha}_5 = \frac{1}{2}\frac{\pi I l}{R^3}$$

$$\tilde{\alpha}_6 = -\frac{1}{32}((81\pi^8 R^{10} + 180\pi^6 R^8 l^2 - 1178\pi^4 R^6 l^4 + 164\pi^4 R^4 f4^2 l^4 - 268\pi^2 R^4 l^6 + 40\pi^2 R^2 l^6 f4^2$$
$$-15R^2 l^8 + 4l^8 f4^2)\pi^5)/(Rl^3(81\pi^8 R^8 + 118\pi^4 R^4 l^4 + 180\pi^6 R^6 l^2 + l^8 + 20l^6 \pi^2 R^2))$$

$$\tilde{\alpha}_7 = -\frac{1}{16}((81\pi^8 R^{10} + 180\pi^6 R^8 l^2 + 118\pi^4 R^6 l^4 + 82\pi^8 f1(t)^2 R^4 l^4 + 20\pi^2 R^4 l^6 + R^2 l^8 + 2f1(t)^2 l^8)$$
$$f1(t)\pi^5)/(Rl^3(81\pi^8 R^8 + 118\pi^4 R^4 l^4 + 180\pi^6 R^6 l^2 + l^8 + 20l^6 \pi^2 R^2))$$

$$\tilde{\alpha}_8 = -\frac{3}{16}(l(41\pi^4 R^4 + 10\pi^2 R^2 l^2 + l^4)\pi^5)/(R(81\pi^8 R^8 + 118\pi^4 R^4 l^4 + 180\pi^6 R^6 l^2 + l^8 + 20l^6 \pi^2 R^2))$$

$$\tilde{\alpha}_9 = -\frac{1}{32}((1296\pi^4 R^8 l^4 + 288\pi^2 R^6 l^6 + 16R^4 l^8)\pi^5)/$$
$$(Rl^3(81\pi^8 R^8 + 118\pi^4 R^4 l^4 + 180\pi^6 R^6 l^2 + l^8 + 20l^6 \pi^2 R^2))$$

Appendix B.3

$$I = \rho h$$

$$\tilde{\tilde{\alpha}}_1 = \frac{1}{2}\frac{\pi^2 D(2\pi^2 l^2 R^2 + \pi^4 R^4 + l^4)}{R^3 l^3}$$

$$\tilde{\tilde{\alpha}}_2 = -\frac{3}{32}\frac{\pi^2 I l w^2}{R}$$

$$\bar{\bar{\alpha}}_3 = \frac{3}{8}\frac{\pi^6 D}{Rl^3}$$

$$\bar{\bar{\alpha}}_4 = -\frac{1}{2}\pi^2 I l {w_0}^2 R$$

$$\bar{\bar{\alpha}}_5 = -\frac{3}{32}(l(41\pi^4R^4 + 10\pi^2R^2l^2 + l^4)EH\pi^6)/(R(81\pi^8R^8 + 118\pi^4R^4l^4 + 180\pi^6R^6l^2 + l^8 + 20\pi^2R^2l^6))$$

$$\bar{\bar{\alpha}}_6 = -\frac{3}{128}((81\pi^8R^{10} + 180\pi^6R^8l^2 - 1178\pi^4R^6l^4 - 268\pi^2R^4l^6 - 15R^2l^8)EH\pi^6)/(R(81\pi^8R^8 + 118\pi^4R^4l^4 + 180\pi^6R^6l^2 + l^8 + 20\pi^2R^2l^6)l^3)$$

$$\bar{\bar{\alpha}}_7 = -\frac{15}{128}(l(41\pi^4R^4 + 10\pi^2R^2l^2 + l^4)EH\pi^6)/(R(81\pi^8R^8 + 118\pi^4R^4l^4 + 180\pi^6R^6l^2 + l^8 + 20\pi^2R^2l)$$

$$\bar{\bar{\alpha}}_8 = -\frac{1}{16}\frac{\pi^6 HER}{l^3}$$

$$\bar{\bar{\alpha}}_9 = -\frac{1}{2}\frac{\pi^6 HElR^3}{\pi^4R^4 + 2\pi^2l^2R^2 + l^4}$$

Appendix B.4

$$b_1 = \frac{3.\varepsilon}{16}$$

$$b_2 = \frac{1}{12}\frac{1}{(\xi^4 + 1 + 2\xi^2)(-1 + v^2)}((-2\varepsilon\xi^8 - 12\varepsilon\xi^4 - 8\varepsilon\xi^6 - 2\varepsilon - 8\varepsilon\xi^2 - 24\xi^4 + 24\xi^4v^2 - 3\varepsilon\bar{w}^2\xi^8 - 3\varepsilon\bar{w}^2\xi^4 - 6\varepsilon\bar{w}^2\xi^6 + 3\varepsilon\bar{w}^2\xi^8v^2 + 3\varepsilon\bar{w}^2\xi^4v^2 + 6\varepsilon\bar{w}^2\xi^6v^2))$$

$$b_3 = \frac{1}{32}((243\upsilon^2\xi^8 - 243\xi^8 - 324\varepsilon\xi^8 - 540\xi^6 + 540\upsilon^2\xi^6 - 720\varepsilon\xi^6 - 492\varepsilon\overline{w}^2\xi^4 + 492\varepsilon\overline{w}^2\xi^4\upsilon^2 + 3534\xi^4$$
$$- 472\varepsilon\xi^4 - 3534\xi^4\upsilon^2 + 120\varepsilon\overline{w}^2\xi^2\upsilon^2 + 804\xi^2 - 80\varepsilon\xi^2 - 804\upsilon^2\xi^2 - 120\varepsilon\overline{w}^2\xi^2 + 45 - 4\varepsilon - 12\varepsilon\overline{w}^2$$
$$+ 12\varepsilon\overline{w}^2\upsilon^2 - 45\upsilon^2)\varepsilon\xi^4)/((81\xi^8 + 118\xi^4 + 180\xi^6 + 1 + 20\xi^2)(-1 + \nu^2))$$

$$b_4 = \frac{15}{32}\frac{\varepsilon^2\xi^4(41\xi^4 + 1 + 10\xi^2)}{81\xi^8 + 118\xi^4 + 180\xi^6 + 1 + 20\xi^2}$$

Appendix B.5

$$A111 = -\frac{1}{2}\frac{l^4R^4m^2n^2\pi^2A(t)^2}{(16n^4l^6R^2 + 64(e\ a)^2n^6l^6)}$$

$$A22 = \frac{1}{4}\frac{R^3.l^4m^2.\pi^2.n^4.A(t)^3}{\left[\begin{array}{l}81.m^4.\pi^4.R^6.l^2 + n^4.l^6.R^2 + 18.m^2.\pi^2.n^2.l^4.R^4 + \\ 729.(ea)^2.m^6.\pi^6.R^6 + 243.(ea)^2.n^2.m^4.\pi^4.l^2.R^4 + 27.(ea)^2.n^4.m^2.\pi^2.l^4.R^2 + (ea)^2.n^6.l^6\end{array}\right]}$$

$$A33 = \frac{1}{2}\frac{R^3.l^4m^2.\pi^2.A(t)(2.R^2 - \frac{n^4.A(t)^2}{2})}{\left[\begin{array}{l}(m^4.\pi^4.l^2.R^6 + n^4.l^6.R^2 + 2.m^2.\pi^2.n^2.l^4.R^4 + (ea)^2.n^6.l^6 + (ea)^2.m^6.\pi^6.R^6 \\ + 3.(ea)^2.n^2.m^4.\pi^4.l^2.R^4 + 3.(ea)^2.n^4.m^2.\pi^2.l^4.R^2)\end{array}\right]}.$$

$$A44 = \frac{1}{4}\frac{R^3.l^4m^2.\pi^2.n^4.A(t)^2W_0}{\left[\begin{array}{l}81.m^4.\pi^4.R^6.l^2 + n^4.l^6.R^2 + 18.m^2.\pi^2.n^2.l^4.R^4 + 729.(ea)^2.m^6.\pi^6.R^6 \\ + 243.(ea)^2.n^2.m^4.\pi^4.l^2.R^4 + 27.(ea)^2.n^4.m^2.\pi^2.l^4.R^2 + (ea)^2.n^6.l^6\end{array}\right]}$$

$$A55 = -\frac{R^4l^4m^2\pi^2n^2A(t)W_0}{16n^4l^6R^2 + 64.(ea)^2n^6l^6}$$

$$A66 = -\frac{1}{4}\frac{R^3.l^4m^2.\pi^2.n^4.A(t)^2W_0}{\left[\begin{array}{l}(m^4.\pi^4.l^2.R^6 + n^4.l^6.R^2 + 2.m^2.\pi^2.n^2.l^4.R^4 + (ea)^2.n^6.l^6 + (ea)^2.m^6.\pi^6.R^6 \\ + 3.(ea)^2.n^2.m^4.\pi^4.l^2.R^4 + 3.(ea)^2.n^4.m^2.\pi^2.l^4.R^2)\end{array}\right]}$$

Appendix B.6

$$b_{11} = (\xi^2 + 1)$$

$$b_{22} = \frac{3.\varepsilon}{16} + \frac{\varepsilon.\mu^2.(\xi^2)}{4}$$

$$b_{33} = \frac{1}{12}((-2\varepsilon - 3\varepsilon\bar{w}^2\xi^{10}\mu^2 - 9\varepsilon\bar{w}^2\xi^8\mu^2 + 3\varepsilon\bar{w}^2\xi^8\nu^2 + 3\varepsilon\bar{w}^2\xi^4\nu^2 + 6\varepsilon\bar{w}^2\xi^6\nu^2 - 96\mu^2\xi^4 - 24\xi^4$$
$$- 52\varepsilon\mu^2\xi^6 - 40\varepsilon\mu^4\xi^8 + 96\xi^4\nu^2\mu^2 - 8\varepsilon\mu^4\xi^{10} - 80\varepsilon\mu^4\xi^4 - 40\varepsilon\mu^4\xi^2 - 68\varepsilon\mu^2\xi^4 - 6\varepsilon\bar{w}^2\xi^6 - 42\varepsilon\mu^2\xi^2$$
$$- 18\varepsilon\mu^2\xi^8 - 2\varepsilon\mu^2\xi^{10} - 80\varepsilon\mu^4\xi^6 - 3\varepsilon\bar{w}^2\xi^8 - 3\varepsilon\bar{w}^2\xi^4 - 9\varepsilon\bar{w}^2\mu^2\xi^6 - 3\varepsilon\bar{w}^2\mu^2\xi^4 - 2\varepsilon\xi^8 - 12\varepsilon\xi^4 - 8\varepsilon\xi^6$$
$$- 10\varepsilon\mu^2 - 8\varepsilon\xi^2 - 8\varepsilon\mu^4 + 24\xi^4\nu^2 + 3\varepsilon\bar{w}^2\xi^4\nu^2\mu^2 + 3\varepsilon\bar{w}^2\xi^{10}u^2\mu^2 + 9\varepsilon\bar{w}^2\xi^8\nu^2\mu^2 + 9\varepsilon\bar{w}^2\xi^6\nu^2\mu^2)) /$$
$$((-1+\nu^2)(\xi^4 + 1 + 2\xi^2 + \mu^2 + \mu^2\xi^6 + 3\mu^2\xi^4 + 3\mu^2\xi^2)(4\mu^2 + 1))$$

$$b_{44} = \frac{1}{32}(\varepsilon\xi^4(45 - 520\varepsilon\mu^2\xi^2 - 3632\varepsilon\mu^2\xi^4 - 920\varepsilon\mu^4\xi^2 - 9144\varepsilon\mu^2\xi^8 - 480\varepsilon\mu^6\xi^2 - 38880\varepsilon\mu^6\xi^{10}$$
$$- 47088\varepsilon\mu^6\xi^8 - 24640\varepsilon\mu^6\xi^6 5232\varepsilon\mu^6\xi^4 - 11664\varepsilon\mu^6\xi^{12} - 2916\varepsilon\mu^4\xi^{12} - 5094\upsilon^2\mu^4\xi^2 + 2430\upsilon^2\mu^2\xi^{10}$$
$$+ 5886u^2\mu^2\xi^8 + 7290\upsilon^2\mu^4\xi^{10} + 8829\upsilon^2\mu^4\xi^8 - 135348\upsilon^2\mu^4\xi^6 - 45675\upsilon^2\mu^4\xi^4 + 2187\upsilon^2\mu^4\xi^{12}$$
$$- 25908\xi^4\upsilon^2\mu^2 - 3240\varepsilon\mu^2\xi^{10} - 30372\upsilon^2\mu^2\xi^6 - 4602\upsilon^2\mu^2\xi^2 - 22680\varepsilon\mu^4\xi^{10} - 9040\varepsilon\mu^2\xi^6$$
$$- 43164\varepsilon\mu^4\xi^8 - 30800\varepsilon\mu^4\xi^6 - 8284\varepsilon\mu^4\xi^4 - 4\varepsilon + 3534\xi^4 - 45v^2 + 804\xi^2 + 234\mu^2 - 540\xi^6$$
$$+ 189\mu^4 - 243\xi^8 + 30372\mu^2\xi^6 + 25908\mu^2\xi^4 + 4602\mu^2\xi^2 - 24\varepsilon\mu^2 - 36\varepsilon\mu^4 - 3534\xi^4\upsilon^2$$
$$- 234\upsilon^2\mu^2 - 16\varepsilon\mu^6 + 540\upsilon^2\xi^6 - 189\upsilon^2\mu^4 + 243\upsilon^2\xi^8 - 324\varepsilon\xi^8 - 472\varepsilon\xi^4 - 720\varepsilon\xi^6 - 80\varepsilon\xi^2$$
$$- 804u^2\xi^2 + 5094\mu^4\xi^2 - 2430\mu^2\xi^{10} - 5886\mu^2\xi^8 - 7290\mu^4\xi^{10} - 8829\mu^4\xi^8 + 135348\mu^4\xi^6$$
$$+ 45675\mu^4\xi^4 - 2187\mu^4\xi^{12} + 3444\varepsilon W^2\xi^4\upsilon^2\mu^2 + 4380\varepsilon W^2\xi^6\upsilon^2\mu^2 + 17520\varepsilon W^2\mu^2\xi^6\upsilon^2$$
$$+ 5904\varepsilon W^2\mu^4\xi^4\upsilon^2 + 720\varepsilon W^2\mu^4\xi^2\upsilon^2 + 660\varepsilon W^2\mu^2\xi^2\upsilon^2 + 492\varepsilon W^2\xi^4\upsilon^2 - 17520\varepsilon W^2\mu^4\xi^6$$
$$- 5904\varepsilon W^2\mu^4\xi^4 - 720\varepsilon W^2\mu^4\xi^2 - 660\varepsilon W^2\mu^2\xi^2 + 120\varepsilon W^2\xi^2\upsilon^2 - 4380\varepsilon w^2\mu^2\xi^6 - 3444\varepsilon W^2\mu^2\xi^4$$
$$+ 60\varepsilon W^2\mu^2\upsilon^2 + 48\varepsilon W^2\mu^4\upsilon - 120\varepsilon W^2\xi^2 - 12\varepsilon W^2)) /$$
$$((\mu^4 + 30\mu^4\xi^2 + 2430\mu^4\xi^{10} + 2943\mu^4\xi^8 + 1540\mu^4\xi^6 + 327\mu^4\xi^4 + 729\mu^4\xi^{12} + 436\mu^2\xi^4 + 50\mu^2\xi^2$$
$$+ 1962\mu^2\xi^8 + 810\mu^2\xi^{10} + 1540\mu^2\xi^6 + 2\mu^2 + 1 + 20\xi^2 + 118\xi^4 + 180\xi^6 + 81\xi^8)(4\mu^2 + 1)(-1 + v^2))$$

$$b_{55} = \frac{5}{32}((\xi^4\varepsilon^2(41\xi^4 + 356\mu^2\xi^4 + 1 + \mu^2 + 10\xi^2 + 123\mu^2\xi^4 + 15\mu^2\xi^2)) /(\mu^4 + 30\mu^4\xi^2 +$$
$$2430\mu^4\xi^8 + 1540\mu^4\xi^6 + 327\mu^4\xi^4 + 436\mu^2\xi^4 + 50\mu^2\xi^2 + 1962\mu^4\xi^8 + 810\mu^2\xi^{10} + 1540\mu^2\xi^6$$
$$+ 2\mu^2 + 1 + 20\xi^2 + 118\xi^4 + 180\xi^6 + 81\xi^8)$$